

1

A search for sparticles in zero lepton final states

2

Russell W. Smith

3

Submitted in partial fulfillment of the

4

requirements for the degree of

5

Doctor of Philosophy

6

in the Graduate School of Arts and Sciences

7

COLUMBIA UNIVERSITY

8

2016

12

ABSTRACT

13

A search for sparticles in zero lepton final states

14

Russell W. Smith

15 TODO : Here's where your abstract will eventually go. The above text is all in the

16 center, but the abstract itself should be written as a regular paragraph on the page,

17 and it should not have indentation. Just replace this text.

19	Contents	i
20	1 Introduction	1
21	2 The Standard Model	5
22	2.1 Overview	5
23	2.2 Field Content	5
24	2.3 Deficiencies of the Standard Model	15
25	3 Supersymmetry	21
26	3.1 Supersymmetric theories : from space to superspace	21
27	3.2 Minimally Supersymmetric Standard Model	24
28	3.3 Phenomenology	30
29	3.4 How SUSY solves the problems with the SM	33
30	3.5 Conclusions	35
31	4 The Large Hadron Collider	37
32	4.1 Basics of Accelerator Physics	37
33	4.2 Accelerator Complex	39
34	4.3 Large Hadron Collider	41
35	4.4 Dataset Delivered by the LHC	43
36	5 The ATLAS detector	49

37	5.1 Inner Detector	49
38	5.2 Calorimeter	51
39	5.3 Muon Spectrometer	51
40	6 The Recursive Jigsaw Technique	53
41	6.1 Razor variables	53
42	6.2 SuperRazor variables	53
43	6.3 The Recursive Jigsaw Technique	53
44	6.4 Variables used in the search for zero lepton SUSY	53
45	7 Table of Contents Title	55
46	8 A search for supersymmetric particles in zero lepton final states	
47	with the Recursive Jigsaw Technique	57
48	8.1 Object reconstruction	57
49	8.2 Signal regions	58
50	8.3 Background estimation	58
51	9 Results	59
52	9.1 Statistical Analysis	59
53	9.2 Signal Region distributions	59
54	9.3 Pull Plots	59
55	9.4 Systematic Uncertainties	59
56	9.5 Exclusion plots	59
57	Conclusion	61
58	9.6 New Section	61
59	Bibliography	63
60	Quantum Field Theory and Symmetries	71

61	Quantum Field Theory	71
62	Symmetries	72
63	Local symmetries	74

Acknowledgements

Dedication

Introduction

Particle physics is a remarkably successful field of scientific inquiry. The ability to precisely predict the properties of a exceedingly wide range of physical phenomena, such as the description of the cosmic microwave background [1, 2], the understanding of the anomalous magnetic dipole moment of the electron [3, 4], and the measurement of the number of weakly-interacting neutrino flavors [5] is truly amazing.

The theory that has allowed this range of predictions is the *Standard Model* of particle physics (SM). The Standard Model combines the electroweak theory of Glashow, Weinberg, and Salam [6–8] with the theory of the strong interactions, as first envisioned by Gell-Mann and Zweig [9, 10]. This quantum field theory (QFT) contains a tiny number of particles, whose interactions describe phenomena up to at least the TeV scale. These particles are manifestations of the fields of the Standard Model, after application of the Higgs Mechanism. The particle content of the SM consists only of the six quarks, the six leptons, the four gauge bosons, and the scalar Higgs boson.

Despite its impressive range of described phenomena, the Standard Model has some theoretical and experimental deficiencies. The SM contains 26 free parameters¹. It would be more theoretically pleasing to understand these free parameters in terms of a more fundamental theory. The major theoretical concern of the Standard Model, as it pertains to this thesis, is the *hierachy problem*[11–15]. The light mass

¹This is the Standard Model corrected to include neutrino masses. These parameters are the fermion masses (6 leptons, 6 quarks), CKM and PMNS mixing angles (8 angles, 2 CP-violating phases), W/Z/Higgs masses (3), the Higgs field expectation value, and the couplings of the strong, weak, and electromagnetic forces (3 α_{force}) .

87 of the Higgs boson (125 GeV) should be quadratically dependent on the scale of UV
 88 physics, due to the quantum corrections from high-energy physics processes. The
 89 most perplexing experimental issue is the existence of *dark matter*, as demonstrated
 90 by galactic rotation curves [16–22]. This data has shown that there exists additional
 91 matter which has not yet been seen interacting with the particles of the Standard
 92 Model. There is no particle in the SM which can act as a candidate for dark matter.

93 Both of these major issues, as well as numerous others, can be solved by the
 94 introduction of *supersymmetry* (SUSY) [15, 23–35]. In supersymmetric theories, each
 95 SM particles has a so-called *superpartner*, or sparticle partner, differing from given SM
 96 particle by 1/2 in spin. These theories solve the hierachy problem, since the quantum
 97 corrections induced from the superpartners exactly cancel those induced by the SM
 98 particles. In addition, these theories are usually constructed assuming R -parity,
 99 which can be thought of as the “charge” of supersymmetry, with SM particles having
 100 $R = 1$ and sparticles having $R = -1$. In collider experiments, since the incoming
 101 SM particles have total $R = 1$, the resulting sparticles are produced in pairs. This
 102 produces a rich phenomenology, which is characterized by significant hadronic activity
 103 and large missing transverse energy (E_T^{miss}), which provide significant discrimination
 104 against SM backgrounds [36].

105 Despite the power of searches for supersymmetry where E_T^{miss} is a primary
 106 discriminating variable, there has been significant interest in the use of other variables
 107 to discriminate against SM backgrounds. These include searches employing variables
 108 such as αT , $M_{T,2}$, and the razor variables (M_R, R^2) [37–47]. In this thesis, we
 109 will present the first search for supersymmetry using the novel Recursive Jigsaw
 110 Reconstruction (RJR) technique. RJR can be considered the conceptual successor
 111 of the razor variables. We impose a particular final state “decay tree” on an events,
 112 which roughly corresponds to a simplified Feynmann diagram in decays containing
 113 weakly-interacting particles. We account for the missing degrees of freedom associated

114 to the weakly-interacting particles by a series of simplifying assumptions, which allow
115 us to calculate our variables of interest at each step in the decay tree. This allows an
116 unprecedented understanding of the internal structure of the decay and the ability to
117 construct additional variables to reject Standard Model backgrounds.

118 This thesis details a search for the superpartners of the gluon and quarks, the
119 gluino and squarks, in final states with zero leptons, with 13.3 fb^{-1} of data using the
120 ATLAS detector. We organize the thesis as follows. The theoretical foundations of
121 the Standard Model and supersymmetry are described in Chapters 2 and 3. The
122 Large Hadron Collider and the ATLAS detector are presented in Chapters 4 and 5.
123 Chapter 5 provides a detailed description of Recursive Jigsaw Reconstruction and a
124 description of the variables used for the particular search presented in this thesis.
125 Chapter 6 presents the details of the analysis, including details of the dataset, object
126 reconstruction, and selections used. In Chapter 7, the final results are presented;
127 since there is no evidence of a supersymmetric signal in the analysis, we present the
128 final exclusion curves in simplified supersymmetric models.

The Standard Model

2.1 Overview

132 A Standard Model is another name for a theory of the internal symmetry group
 133 $SU(3)_C \otimes SU(2)_L \otimes U(1)_Y$, with its associated set of parameters. *The* Standard
 134 Model refers specifically to a Standard Model with the proper parameters to describe
 135 the universe. The SM is the culmination of years of work in both theoretical
 136 and experimental particle physics. In this thesis, we take the view that theorists
 137 construct a model with the field content and symmetries as inputs, and write down the
 138 most general Lagrangian consistent with those symmetries. Assuming this model is
 139 compatible with nature (in particular, the predictions of the model are consistent with
 140 previous experiments), experimentalists are responsible measuring the parameters of
 141 this model This will be applicable for this chapter and the following one.

cite

142 Additional theoretical background is in 9.6. The philosophy and notations are
 143 inspired by [48, 49].

2.2 Field Content

The Standard Model field content is

$$\begin{aligned}
 \text{Fermions} &: Q_L(3, 2)_{+1/3}, U_R(3, 1)_{+4/3}, D_R(3, 1)_{-2/3}, L_L(1, 2)_{-1}, E_R(1, 1)_{-2} \\
 \text{Scalar (Higgs)} &: \phi(1, 2)_{+1} \\
 \text{Vector Fields} &: G^\mu(8, 1)_0, W^\mu(1, 3)_0, B^\mu(1, 1)_0
 \end{aligned} \tag{2.1}$$

145 where the $(A, B)_Y$ notation represents the irreducible representation under $SU(3)$
 146 and $SU(2)$, with Y being the electroweak hypercharge. Each of these fermion fields
 147 has an additional index, representing the three generation of fermions.

148 We observed that Q_L, U_R , and D_R are triplets under $SU(3)_C$; these are the *quark*
 149 fields. The *color* group, $SU(3)_C$ is mediated by the *gluon* field $G^\mu(8, 1)_0$, which has
 150 8 degrees of freedom. The fermion fields $L_L(1, 2)_{-1}$ and $E_R(1, 1)_{-2}$ are singlets under
 151 $SU(3)_C$; we call them the *lepton* fields.

152 Next, we note the “left-handed” (“right-handed”) fermion fields, denoted by L (R)
 153 subscript, The left-handed fields form doublets under $SU(2)_L$. These are mediated
 154 by the three degrees of freedom of the “W” fields $W^\mu(1, 3)_0$. These fields only act
 155 on the left-handed particles of the Standard Model. This is the reflection of the
 156 “chirality” of the Standard Model; the left-handed and right-handed particles are
 157 treated differently by the electroweak forces. The right-handed fields, U_R, D_R , and
 158 E_R , are singlets under $SU(2)_L$.

159 The $U(1)_Y$ symmetry is associated to the $B^\mu(1, 1)_0$ boson with one degree of
 160 freedom. The charge Y is known as the electroweak hypercharge.

161 To better understand the phenomenology of the Standard Model, let us investigate
 162 each of the *sectors* of the Standard Model separately.

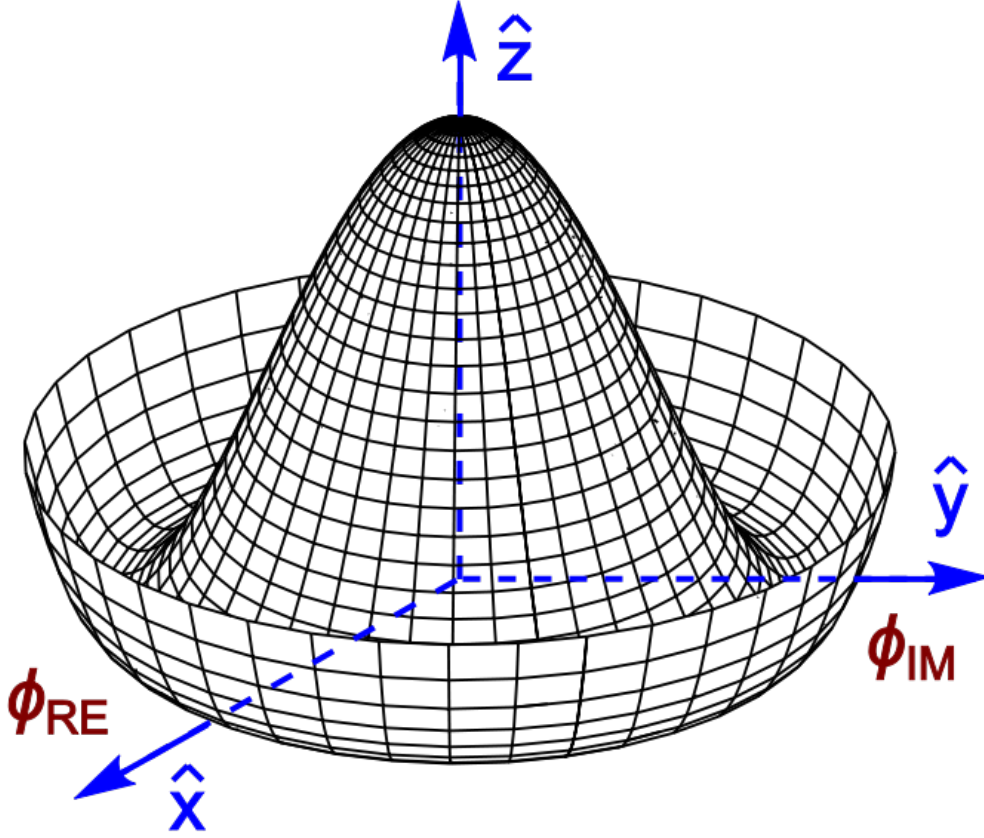
163 Electroweak sector

The electroweak sector refers to the $SU(2)_L \otimes U(1)_Y$ portion of the Standard
 Model gauge group. Following our philosophy of writing all gauge-invariant and
 renormalizable terms, the electroweak Lagrangian can be written as

$$\mathcal{L} = W_a^{\mu\nu} W_{\mu\nu}^a + B^{\mu\nu} B_{\mu\nu} + (D^\mu \phi)^\dagger D_\mu \phi - \mu^2 \phi^\dagger \phi - \lambda(\phi^\dagger \phi)^2. \quad (2.2)$$

where $W_a^{\mu\nu}$ are the three ($a = 1, 2, 3$) gauge bosons associated to the $SU(2)_L$ gauge
 group, $B^{\mu\nu}$ is the one gauge boson of the $U(1)_Y$ gauge group, and ϕ is the complex

Figure 2.1: Sombrero potential



Higgs multiplet. The covariant derivative D^μ is given by

$$D^\mu = \partial^\mu + \frac{ig}{2} W_a^\mu \sigma_a + \frac{ig'}{2} B^\mu \quad (2.3)$$

where $i\sigma_a$ are the Pauli matrices times the imaginary constant, which are the generators for $SU(2)_L$, and g and g' are the $SU(2)_L$ and $U(1)_Y$ coupling constants, respectively. The field strength tensors $W_a^{\mu\nu}$ and $B^{\mu\nu}$ are given by the commutator of the covariant derivative associated to each field

$$B^{\mu\nu} = \partial^\mu B^\nu - \partial^\nu B^\mu \quad (2.4)$$

$$W_a^{\mu\nu} = \partial^\mu W_a^\nu - \partial^\nu W_a^\mu - g\epsilon_{abc} W_a^\mu W_b^\nu, \quad i = 1, 2, 3$$

165 The terms in the Lagrangian 2.2 proportional to μ^2 and λ make up the “Higgs
 166 potential” [50]. As normal (see Appendix 9.6), we restrict $\lambda > 0$ to guarantee our
 167 potential is bounded from below, and we also require $\mu^2 < 0$, which gives us the
 168 standard “sombbrero” potential shown in 2.1.

This potential has infinitely many minima at $\langle \phi \rangle = \sqrt{2m/\lambda}$; the ground state is
spontaneously broken by the choice of ground state, which induces a vacuum expectation
 value (VEV). Without loss of generality, we can choose the Higgs field ϕ to point in
 the real direction, and write the Higgs field ϕ in the following form :

$$\phi = \frac{1}{\sqrt{2}} \exp\left(\frac{i}{v} \sigma_a \theta_a\right) \begin{pmatrix} 0 \\ v + h(x) \end{pmatrix}. \quad (2.5)$$

We choose a gauge to rotate away the dependence on θ_a , such that we can write
 simply

$$\phi = \frac{1}{\sqrt{2}} \begin{pmatrix} 0 \\ v + h(x) \end{pmatrix}. \quad (2.6)$$

Now, we can see how the masses of the vector bosons are generated from the
 application of the Higgs mechanism. We plug Eq.2.6 back into the electroweak
 Lagrangian, and only showing the relevant mass terms in the vacuum state where
 $h(x) = 0$ see that (dropping the Lorentz indices) :

$$\begin{aligned} \mathcal{L}_M &= \frac{1}{8} \left| \begin{pmatrix} gW_3 + g'B & g(W_1 - iW_2) \\ g(W_1 + iW_2) & -gW_3 + g'B \end{pmatrix} \begin{pmatrix} 0 \\ v \end{pmatrix} \right|^2 \\ &= \frac{g^2 v^2}{8} \left[W_1^2 + W_2^2 + \left(\frac{g'}{g} B - W_3\right)^2 \right] \end{aligned} \quad (2.7)$$

Defining the *Weinberg* angle $\tan(\theta_W) = g'/g$ and the following *physical* fields :

$$W^\pm = \frac{1}{\sqrt{2}}(W_1 \mp iW_2) \quad (2.8)$$

$$Z^0 = \cos \theta_W W_3 - \sin \theta_W B$$

$$A^0 = \sin \theta_W W_3 + \cos \theta_W B$$

we can write the piece of the Lagrangian associated to the vector boson masses as

$$\mathcal{L}_{M_V} = \frac{1}{4}g^2v^2W^+W^- + \frac{1}{8}(g^2 + g'^2)v^2Z^0Z^0. \quad (2.9)$$

and we have the following values of the masses for the vector bosons :

$$\begin{aligned} m_W^2 &= \frac{1}{4}v^2g^2 \\ m_Z^2 &= \frac{1}{4}v^2(g^2 + g'^2) \\ m_A^2 &= 0 \end{aligned} \quad (2.10)$$

169 We thus see how the Higgs mechanism gives rise to the masses of the W^\pm and Z
 170 boson in the Standard Model; the mass of the photon is zero, as expected. The
 171 $SU(2)_L \otimes U(1)_Y$ symmetry of the initially massless $W_{1,2,3}$ and B fields is broken to
 172 the $U(1)_{EM}$. Of the four degrees of freedom in the complex Higgs doublet, three are
 173 “eaten” when we give mass to the W^\pm and Z_0 , while the other degree of freedom is
 174 the Higgs particle, as found in 2012 by the ATLAS and CMS collaborations [51, 52].

175 Quantum Chromodynamics

Quantum chromodynamics (or the theory of the *strong* force) characterizes the behavior of *colored* particles, collectively known as *partons*. The partons of the Standard Model are the (fermionic) quarks, and the (bosonic) gluons. The strong force is governed by $SU(3)_C$, an unbroken symmetry in the Standard Model, which implies the gluon remains massless. Defining the covariant derivative for QCD as

$$D^\mu = \partial^\mu + ig_s G_a^\mu L_a, a = 1, \dots, 8 \quad (2.11)$$

where L_a are the generators of $SU(3)_C$, and g_s is the coupling constant of the strong force. The QCD Lagrangian then is given by

$$\mathcal{L}_{\text{QCD}} = i\bar{\psi}_f D_\mu \gamma^\mu \psi_f - \frac{1}{4} G_{a,\mu\nu} G_a^{\mu\nu} \quad (2.12)$$

where the summation over f is for quarks *families*, and $G_a^{\mu\nu}$ is the gluon field strength tensor, given by

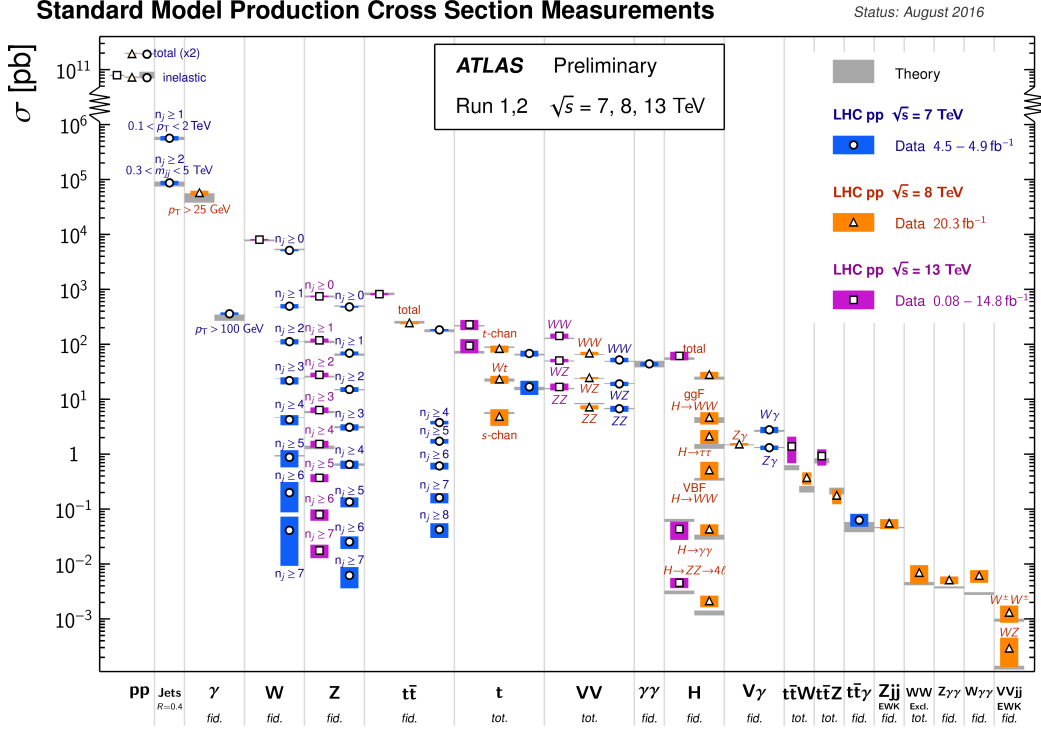
$$G_a^{\mu\nu} = \partial^\mu G_a^\nu - \partial^\nu G_a^\mu - g_s f^{abc} G_b^\mu G_c^\nu, a, b, c = 1, \dots, 8 \quad (2.13)$$

176 where f^{abc} are the structure constants of $SU(3)_C$, which are analogous to ϵ_{abc} for
 177 $SU(2)_L$. The kinetic term for the quarks is contained in the standard ∂_μ term, while
 178 the field strength term contains the interactions between the quarks and gluons, as
 179 well as the gluon self-interactions.

180 Written down in this simple form, the QCD Lagrangian does not seem much
 181 different from the QED Lagrangian, with the proper adjustments for the different
 182 group structures. The gluon is massless, like the photon, so one could naïvely expect
 183 an infinite range force, and it pays to understand why this is not the case. The
 184 reason for this fundamental difference is the gluon self-interactions arising in the
 185 field strength tensor term of the Lagrangian. This leads to the phenomena of *color*
 186 *confinement*, which describes how one only observes color-neutral particles alone in
 187 nature. In contrast to the electromagnetic force, particles which interact via the
 188 strong force experience a *greater* force as the distance between the particles increases.
 189 At long distances, the potential is given by $V(r) = -kr$. At some point, it is more
 190 energetically favorable to create additional partons out of the vacuum than continue
 191 pulling apart the existing partons, and the colored particles undergo *fragmentation*.
 192 This leads to *hadronization*. Bare quarks and gluons are actually observed as sprays
 193 of hadrons (primarily kaons and pions); these sprays are known as *jets*, which are
 194 what are observed by experiments.

195 It is important to recognize the importance of understanding these QCD inter-
 196 actions in high-energy hadron colliders such as the LHC. Since protons are hadrons,
 197 proton-proton collisions such as those produced by the LHC are primarily governed by
 198 the processes of QCD. In particular, by far the most frequent process observed in LHC
 199 experiments is dijet production from gluon-gluon interactions (see Fig.2.2). These

Figure 2.2: Cross-sections of various Standard Model processes



gluons that interact are part of the *sea* particles inside the proton; the simple $p = uud$ model does not apply. The main *valence* uud quarks are constantly interacting via gluons, which can themselves radiate gluons or split into quarks, and so on. A more useful understanding is given by the colloquially-known *bag* model [53, 54], where the proton is seen as a “bag” of (in principle) infinitely many partons, each with energy $E < \sqrt{s} = 6.5$ TeV. One then collides this (proton) bag with another, and views the products of this very complicated collision, where calculations include many loops in nonperturbative QCD calculations.

Fortunately, we are generally saved by the QCD factorization theorems [55]. This allows one to understand the hard (i.e. short distance or high energy) $2 \rightarrow 2$ parton process using the tools of perturbative QCD, while making series of approximations known as a *parton shower* model to understand the additional corrections from nonperturbative QCD. We will discuss the reconstruction of jets by experiments in Ch.5.

214 Fermions

215 We will now look more closely at the fermions in the Standard Model [56].

216 As noted earlier in Sec.2.2, the fermions of the Standard Model can be first
217 distinguished between those that interact via the strong force (quarks) and those
218 which do not (leptons).

There are six leptons in the Standard Model, which can be placed into three *generations*.

$$\begin{pmatrix} e \\ \nu_e \end{pmatrix}, \begin{pmatrix} \mu \\ \nu_\mu \end{pmatrix}, \begin{pmatrix} \tau \\ \nu_\tau \end{pmatrix} \quad (2.14)$$

219 There is the electron (e), muon (μ), and tau (τ), each of which has an associated
220 neutrino (ν_e, ν_μ, ν_τ). Each of the so-called charged (“electron-like”) leptons has
221 electromagnetic charge -1 , while the neutrinos all have $q_{EM} = 0$.

222 Often in an experimental context, lepton is used to denote the stable electron
223 and metastable muon, due to their striking experimental signatures. Taus are often
224 treated separately, due to their much shorter lifetime of $\tau_\tau \sim 10^{-13}s$; these decay
225 through hadrons or the other leptons, so often physics analyses at the LHC treat
226 them as jets or leptons, as will be done in this thesis.

227 As the neutrinos are electrically neutral, nearly massless, and only interact via the
228 weak force, it is quite difficult to observe them directly. Since LHC experiments rely
229 overwhelmingly on electromagnetic interactions to observe particles, the presence of
230 neutrinos is not observed directly. Neutrinos are instead observed by the conservation
231 of four-momentum in the plane transverse to the proton-proton collisions, known as
232 *missing transverse energy*.

There are six quarks in the Standard Model : up, down, charm, strange, top, and bottom. Quarks are similar organized into three generations :

$$\begin{pmatrix} u \\ d \end{pmatrix}, \begin{pmatrix} c \\ s \end{pmatrix}, \begin{pmatrix} t \\ b \end{pmatrix} \quad (2.15)$$

233 where we speak of “up-like” quarks and “down-like” quarks.

234 Each up-like quark has charge $q_{up} = 2/3$, while the down-like quarks have $q_{down} =$
235 $-1/3$. At the high energies of the LHC, one often makes the distinction between
236 the light quarks (u, d, c, s), the bottom quark, and top quark. In general, due to
237 the hadronization process described above, the light quarks, with masses $m_q < \sim$
238 1.5GeV are indistinguishable by LHC experiments. Their hadronic decay products
239 generally have long lifetimes and they are reconstructed as jets.¹ The bottom quark
240 hadronizes primarily through the B -mesons, which generally travels a short distance
241 before decaying to other hadrons. This allows one to distinguish decays via b -quarks
242 from other jets; this procedure is known as *b-tagging* and will be discussed more in
243 Ch.5. Due to its large mass, the top quark decays before it can hadronize; there
244 are no bound states associated to the top quark. The top is of particular interest at
245 the LHC; it has a striking signature through its most common decay mode $t \rightarrow Wb$.
246 Decays via tops, especially $t\bar{t}$ are frequently an important signal decay mode, or an
247 important background process.

248 Interactions in the Standard Model

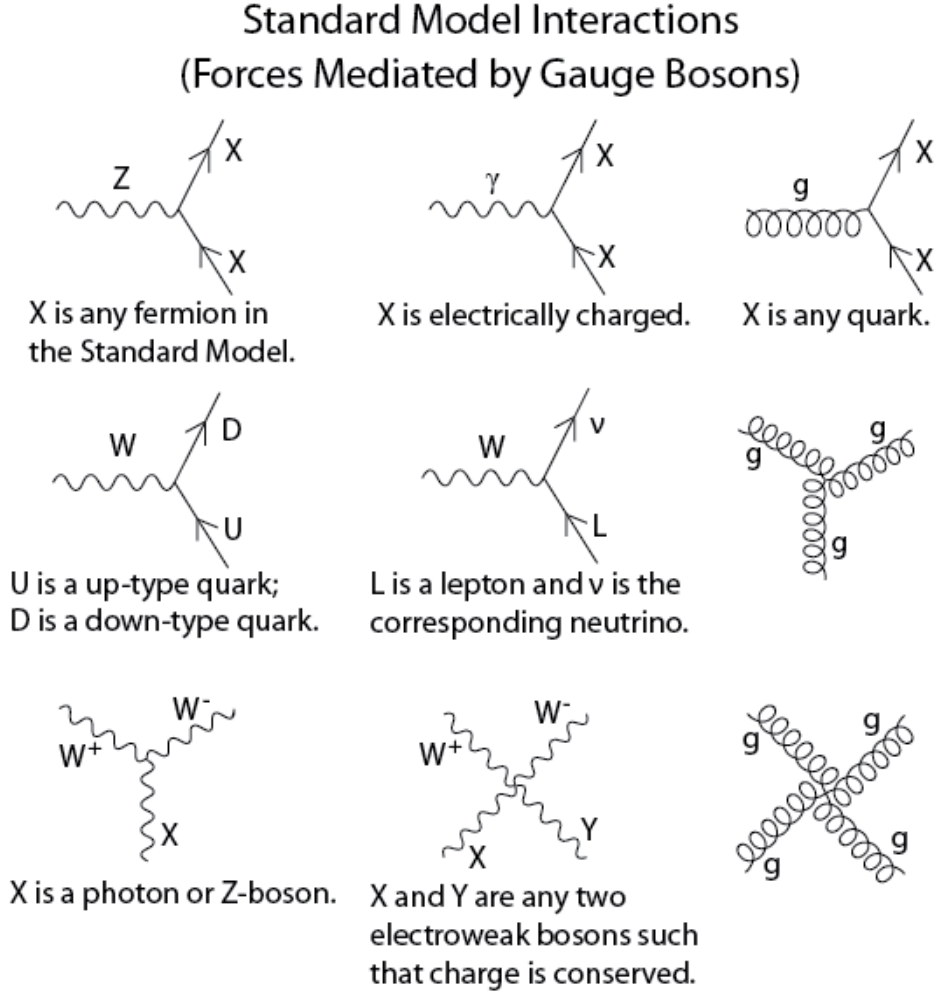
249 We briefly overview the entirety of the fundamental interactions of the Standard
250 Model; these can also be found in 2.3.

251 The electromagnetic force, mediated by the photon, interacts with via a three-
252 point coupling all charged particles in the Standard Model. The photon thus interacts
253 with all the quarks, the charged leptons, and the charged W^\pm bosons.

254 The weak force is mediated by three particles : the W^\pm and the Z^0 . The Z^0 can
255 interact with all fermions via a three-point coupling. A real Z_0 can thus decay to
256 a fermion-antifermion pair of all SM fermions except the top quark, due to its large

¹In some contexts, charm quarks are also treated as a separate category, although it is quite difficult to distinguish charm quarks from the other light quarks.

Figure 2.3: The interactions of the Standard Model



257 mass. The W^\pm has two important three-point interactions with fermions. First, the
 258 W^\pm can interact with an up-like quark and a down-like quark; an important example
 259 in LHC experiments is $t \rightarrow Wb$. The coupling constants for these interactions are
 260 encoded in the unitary matrix known as the Cabibbo–Kobayashi–Maskawa (CKM)
 261 matrix [57, 58], and are generally known as flavor-changing interactions. Secondly,
 262 the W^\pm interacts with a charged lepton and its corresponding neutrino. In this case,
 263 the unitary matrix that corresponds to CKM matrix for quarks is the identity matrix,
 264 which forbids (fundamental) vertices such as $\mu \rightarrow We$. For leptons, instead this is
 265 a two-step process : $\mu \rightarrow \nu_\mu u W \rightarrow \nu_\mu u \bar{\nu}_e e$. Finally, there are the self-interactions

266 of the weak gauge bosons. There is a three-point and four-point interaction; all
 267 combinations are allowed which conserve electric charge.

268 The strong force is mediated by the gluon, which as discussed above also carries
 269 the strong color charge. There is the fundamental three-point interaction, where a
 270 quark radiates a gluon. Additionally, there are the three-point and four-point gluon-
 271 only interactions.

272 2.3 Deficiencies of the Standard Model

273 At this point, it is quite easy to simply rest on our laurels. This relatively simple
 274 theory is capable of explaining a very wide range of phenomenom, which ultimately
 275 break down only to combinations of nine diagrams shown in Fig.2.3. Unfortunately,
 276 there are some unexplained problems with the Standard Model. We cannot go
 277 through all of the potential issues in this thesis, but we will motivate the primary
 278 issues which naturally lead one to *supersymmetry*, as we will see in Ch.3.

The Standard Model has many free paramaters; see Table 2.1 In general, we prefer
 models with less free parameters. A great example of this fact, and the primary
 experimental evidence for EWSB, is the relationship between the couplings of the
 weak force and the masses of the gauge bosons of the weak force :

$$\rho \equiv \frac{m_W^2}{m_Z^2 \cos^2 \theta_W} \stackrel{?}{=} 1 \quad (2.16)$$

279 where ? indicates that this is a testable prediction of the Standard Model (in
 280 particular, that the gauge bosons gain mass through EWSB). This relationship has
 281 been measured within experimental and theoretical predictions. We would like to
 282 produce additional such relationships, which would exist if the Standard Model is a
 283 low-energy approximation of some other theory.

284 An additional issue is the lack of *gauge coupling unification*. The couplings of
 285 any quantum field theory “run” as a function of the distance scales (or inversely,

Table 2.1: Parameters of the Standard Model. For values dependent on the renormalization scheme, we use a combination of the on-shell normalization scheme [59–62] and modified minimal subtraction scheme with $m_{\bar{M}S}$ as indicated in the table[63]

m_e	Electron mass	511 keV
m_μ	Muon mass	105.7 MeV
m_τ	Tau mass	1.78 GeV
m_u	Up quark mass	1.9 MeV ($m_{\bar{M}S} = 2GeV$)
m_d	Down quark mass	4.4 MeV ($m_{\bar{M}S} = 2GeV$)
m_s	Strange quark mass	87 MeV ($m_{\bar{M}S} = 2GeV$)
m_c	Charm quark mass	1.32 GeV ($m_{\bar{M}S} = m_c$)
m_b	Bottom quark mass	4.24 GeV ($m_{\bar{M}S} = m_b$)
m_t	Top quark mass	172.7 GeV (on-shell renormalization)
θ_{12} CKM	12-mixing angle	13.1°
θ_{23} CKM	23-mixing angle	2.4°
θ_{13} CKM	13-mixing angle	0.2°
δ CKM	CP-violating Phase	0.995
g'	U(1) gauge coupling	0.357 ($m_{\bar{M}S} = m_Z$)
g	SU(2) gauge coupling	0.652 ($m_{\bar{M}S} = m_Z$)
g_s	SU(3) gauge coupling	1.221 ($m_{\bar{M}S} = m_Z$)
θ_{QCD}	QCD vacuum angle	~ 0
VEV	Higgs vacuum expectation value	246 GeV
m_H	Higgs mass	125 GeV

energy scales) of the theory. The idea is closely related to the unification of the electromagnetic and weak forces at the so-called *electroweak scale* of $O(100 \text{ GeV})$. One would hope this behavior was repeated between the electroweak forces and the strong force at some suitable energy scale. The Standard Model does automatically not exhibit this behavior, as we can see in Fig.2.4.

The most significant problem with the Standard Model is the *hierarchy problem*. In its most straightforward incarnation, the Higgs scalar field is subject to quantum corrections through loop diagrams, as shown in Fig.2.5. For demonstration, we use the contributions from the top quark, since the top quark has the largest Higgs Yukawa coupling due to its large mass. In general, we should expect these corrections to quadratically dependent on the scale of the ultraviolet physics, Λ . Briefly assume there is no new physics before the Planck scale of gravity, $\Lambda_{\text{Planck}} = 10^{19} \text{ GeV}$. In this

Figure 2.4: The running of Standard Model gauge couplings. The Standard Model couplings do not unify at high energies, which indicates it cannot completely describe nature through the Planck scale.

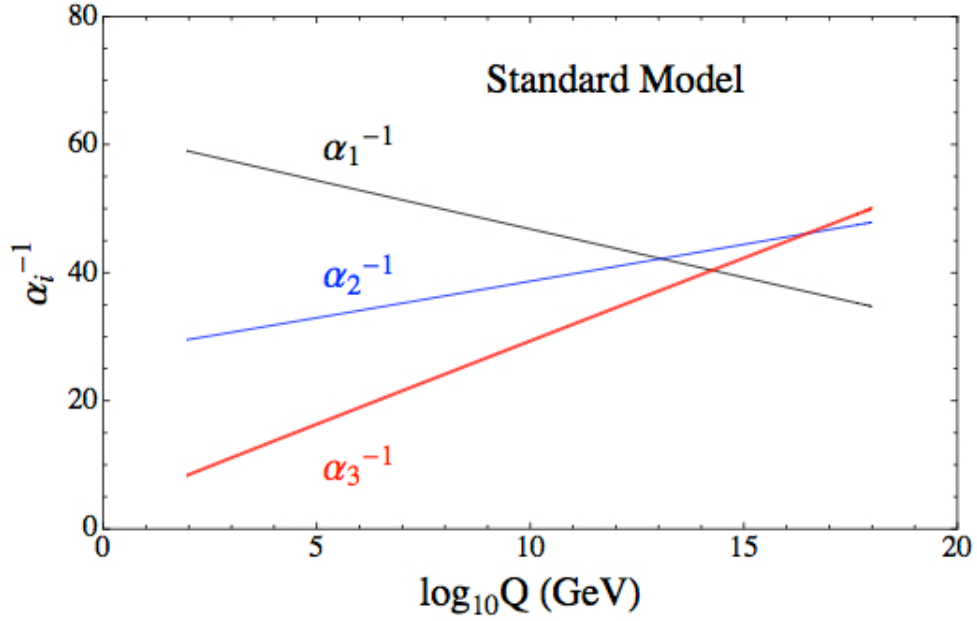
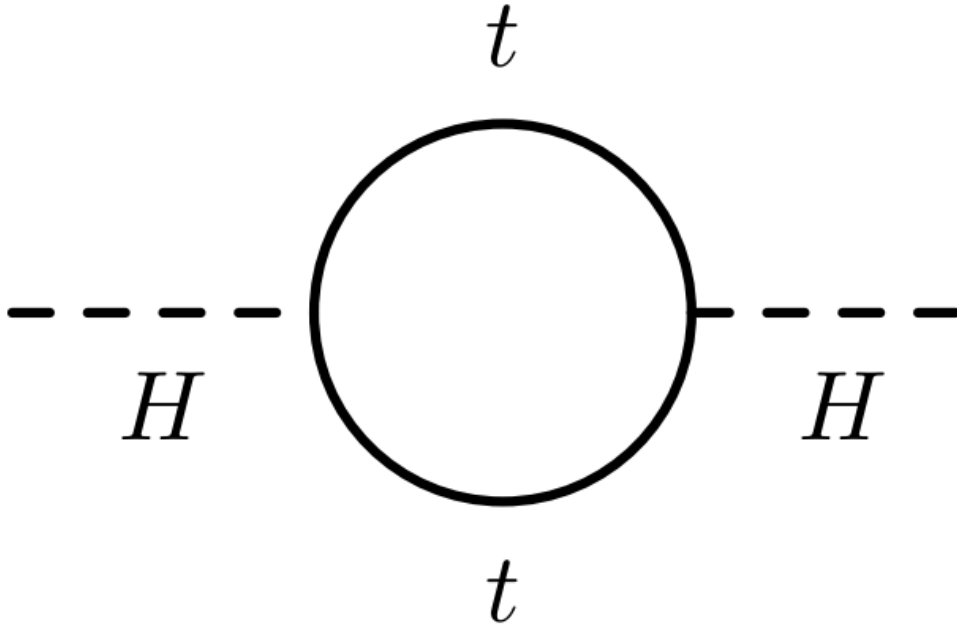


Figure 2.5: The dominant quantum loop correction to the Higgs mass in the Standard Model.



case, we expect the corrections to the Higgs mass like

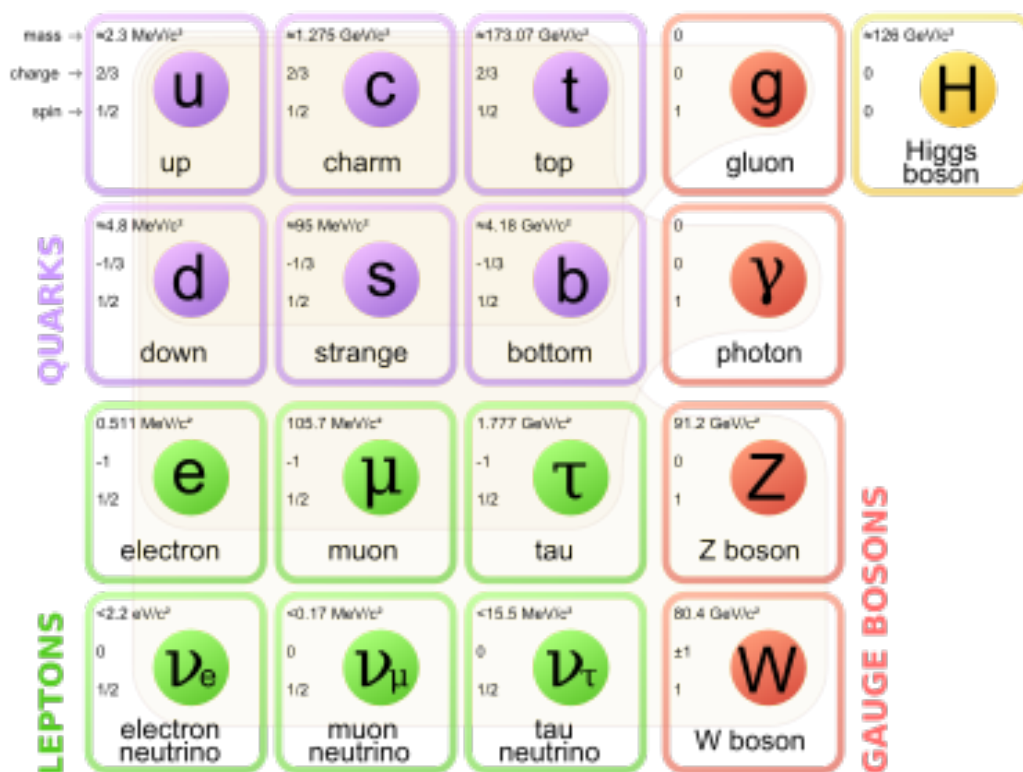
$$\delta m_H^2 \approx \left(\frac{m_t}{8\pi^2 \langle \phi \rangle_{VEV}} \right)^2 \Lambda_{Planck}^2. \quad (2.17)$$

291 To achieve the miraculous cancellation required to get the observed Higgs mass of
292 125 GeV, one needs to then set the bare Higgs mass m_0 , our input to the Standard
293 Model Lagrangian, itself to a *precise* value $\sim 10^{19}$ GeV. This extraordinary level of
294 parameter finetuning is quite undesirable, and within the framework of the Standard
295 Model, there is little that can be done to alleviate this issue.

296 An additional concern, of a different nature, is the lack of a *dark matter* candidate
297 in the Standard Model. Dark matter was discovered by observing galactic rotation
298 curves, which showed that much of the matter that interacted gravitationally was
299 invisible to our (electromagnetic) telescopes [16–22]. The postulation of the existence
300 of dark matter, which interacts at least through gravity, allows one to understand
301 these galactic rotation curves. Unfortunately, no particle in the Standard Model could
302 possibly be the dark matter particle. The only candidate truly worth another look is
303 the neutrino, but it has been shown that the neutrino content of the universe is simply
304 too small to explain the galactic rotation curves [22, 64]. The experimental evidence
305 from the galactic rotations curves thus show there *must* be additional physics beyond
306 the Standard Model, which is yet to be understood.

307 In the next chapter, we will see how these problems can be alleviated by the theory
308 of supersymmetry.

Figure 2.6: Particles of the Standard Model



Supersymmetry

311 This chapter will introduce supersymmetry (SUSY) [15, 23–35]. We will begin by
 312 introducing the concept of a *superspace*, and discuss some general ingredients of
 313 supersymmetric theories. This will include a discussion of how the problems with the
 314 Standard Model described in Ch.2 are naturally fixed by these theories.

315 The next step is to discuss the particle content of the *Minimally Supersymmetric*
 316 *Standard Model* (MSSM). As its name implies, this theory contains the minimal
 317 additional particle content to make Standard Model supersymmetric. We then discuss
 318 the important phenomenological consequences of this theory, especially as it would
 319 be observed in experiments at the LHC.

320 **3.1 Supersymmetric theories : from space to** 321 **superspace**

322 **Coleman-Mandula “no-go” theorem**

323 We begin the theoretical motivation for supersymmetry by citing the “no-go” theorem
 324 of Coleman and Mandula [65]. This theorem forbids *spin-charge unification*; it
 325 states that all quantum field theories which contain nontrivial interactions must be
 326 a direct product of the Poincaré group of Lorentz symmetries, the internal product
 327 from of gauge symmetries, and the discrete symmetries of parity, charge conjugation,
 328 and time reversal. The assumptions which go into building the Coleman-Mandula

theorem are quite restrictive, but there is one unique way out, which has become known as *supersymmetry* [26, 66]. In particular, we must introduce a *spinorial* group generator Q . Alternatively, and equivalently, this can be viewed as the addition of anti-commuting coordinates; space plus these new anti-commuting coordinates is then called *superspace* [67]. We will not investigate this view in detail, but it is also a quite intuitive and beautiful way to construct supersymmetry[15].

Supersymmetry transformations

A *supersymmetric* transformation Q transforms a bosonic state into a fermionic state, and vice versa :

$$Q |\text{Fermion}\rangle = |\text{Boson}\rangle \quad (3.1)$$

$$Q |\text{Boson}\rangle = |\text{Fermion}\rangle \quad (3.2)$$

To ensure this relation holds, Q must be an anticommuting spinor. Additionally, since spinors are inherently complex, Q^\dagger must also be a generator of the supersymmetry transformation. Since Q and Q^\dagger are spinor objects (with $s = 1/2$), we can see that supersymmetry must be a spacetime symmetry. The Haag-Lopuszanski-Sohnius extension [66] of the Coleman-Mandula theorem [65] is quite restrictive about the forms of such a symmetry. Here, we simply write the (anti-) commutation relations [15] :

$$Q_\alpha, Q_\alpha^\dagger = -2\sigma_{\alpha\dot{\alpha}\mu} P_\mu \quad (3.3)$$

$$Q_\alpha, Q_\beta = Q_\alpha^\dagger, Q_\beta^\dagger = 0 \quad (3.4)$$

$$[P^\mu, Q_\alpha] = [P^\mu, Q_\alpha^\dagger] = 0 \quad (3.5)$$

338 Supermultiplets

339 In a supersymmetric theory, we organize single-particle states into irreducible
340 representations of the supersymmetric algebra which are known as *supermultiplets*.
341 Each supermultiplet contains a fermion state $|F\rangle$ and a boson state $|B\rangle$; these two
342 states are known as *superpartners*. These are related by some combination of
343 Q and Q^\dagger , up to a spacetime transformation. Q and Q^\dagger commute with the mass-
344 squared operator $-P^2$ and the operators corresponding to the gauge transformations
345 [15]; in particular, the gauge interactions of the Standard Model. In an unbroken
346 supersymmetric theory, this means the states $|F\rangle$ and $|B\rangle$ have exactly the same mass,
347 electromagnetic charge, electroweak isospin, and color charges. One can also prove
348 [15] that each supermultiplet contains the exact same number of bosonic (n_B) and
349 fermion (n_F) degrees of freedom. We now explore the possible types of supermultiples
350 one can find in a renormalizable supersymmetric theory.

351 Since each supermultiplet must contain a fermion state, the simplest type of
352 supermultiplet contains a single Weyl fermion state ($n_F = 2$) which is paired with
353 $n_B = 2$ scalar bosonic degrees of freedom. This is most conveniently constructed as
354 single complex scalar field. We call this construction a *scalar supermultiplet* or *chiral*
355 *supermultiplet*. The second name is indicative; only chiral supermultiplets can contain
356 fermions whose right-handed and left-handed components transform differently under
357 the gauge interactions (as of course happens in the Standard Model).

358 The second type of supermultiplet we construct is known as a *gauge* supermul-
359 tiplet. We take a spin-1 gauge boson (which must be massless due to the gauge
360 symmetry, so $n_B = 2$) and pair this with a single massless Weyl spinor¹. The gauge
361 bosons transform as the adjoint representation of their respective gauge groups;
362 their fermionic partners, which are known as gauginos, must also. In particular,
363 the left-handed and right-handed components of the gaugino fermions have the same

¹Choosing an $s = 3/2$ massless fermion leads to nonrenormalizable interactions.

364 gauge transformation properties.

365 Excluding gravity, this is the entire list of supermultiplets which can participate
366 in renormalizable interactions in what is known as $N = 1$ supersymmetry. This
367 means there is only one copy of the supersymmetry generators Q and Q^\dagger . This is
368 essentially the only “easy” phenomenological choice, since it is the only choice in four
369 dimensions which allows for the chiral fermions and parity violations built into the
370 Standard Model, and we will not look further into $N > 1$ supersymmetry in this thesis.

371 The primary goal, after understanding the possible structures of the multiplets
372 above, is to fit the Standard Model particles into a multiplet, and therefore make
373 predictions about their supersymmetric partners. We explore this in the next section.

374 **3.2 Minimally Supersymmetric Standard Model**

375 To construct what is known as the MSSM [[susyPrimer](#), [68–71](#)], we need a few
376 ingredients and assumptions. First, we match the Standard Model particles with
377 their corresponding superpartners of the MSSM. We will also introduce the naming
378 of the superpartners (also known as *sparticles*). We discuss a very common additional
379 restraint imposed on the MSSM, known as R -parity. We also discuss the concept of
380 soft supersymmetry breaking and how it manifests itself in the MSSM.

381 **Chiral supermultiplets**

382 The first thing we deduce is directly from Sec.???. The bosonic superpartners
383 associated to the quarks and leptons *must* be spin 0, since the quarks and leptons must
384 be arranged in a chiral supermultiplet. This is essentially the note above, since the
385 chiral supermultiplet is the only one which can distinguish between the left-handed
386 and right-handed components of the Standard Model particles. The superpartners of
387 the quarks and leptons are known as *squarks* and *sleptons*, or *sfermions* in aggregate.

388 (for “scalar quarks”, “scalar leptons”, and “scalar fermion”²). The “s-” prefix
389 can also be added to the individual quarks i.e. *selectron*, *sneutrino*, and *stop*. The
390 notation is to add a \sim over the corresponding Standard Model particle i.e. \tilde{e} , the
391 selectron is the superpartner of the electron. The two-component Weyl spinors of the
392 Standard Model must each have their own (complex scalar) partner i.e. e_L, e_R have
393 two distinct partners : \tilde{e}_L, \tilde{e}_R . As noted above, the gauge interactions of any of the
394 sfermions are identical to those of their Standard Model partners.

Due to the scalar nature of the Higgs, it must obviously lie in a chiral supermultiplet. To avoid gauge anomalies and ensure the correct Yukawa couplings to the quarks and leptons[15], we must add additional Higgs bosons to any supersymmetric theory. In the MSSM, we have two chiral supermultiplets. The SM (SUSY) parts of the multiplets are denoted $H_u(\tilde{H}_u)$ and $H_d(\tilde{H}_d)$. Writing out H_u and H_d explicitly:

$$H_u = \begin{pmatrix} H_u^+ \\ H_u^0 \end{pmatrix} \quad (3.6)$$

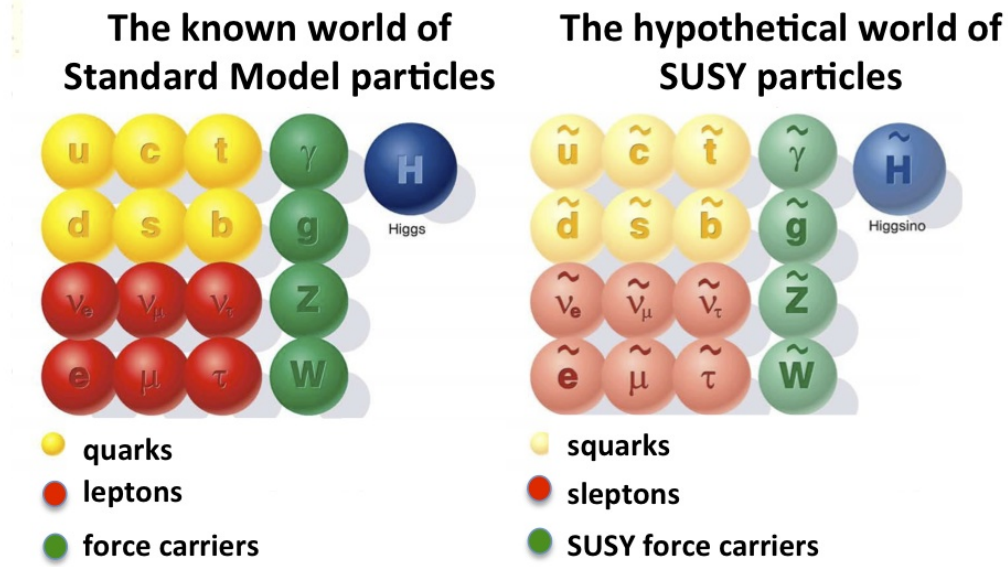
$$H_d = \begin{pmatrix} H_d^0 \\ H_d^- \end{pmatrix} \quad (3.7)$$

$$(3.8)$$

395 we see that H_u looks very similar to the SM Higgs with $Y = 1$, and H_d is symmetric
396 to this with $+$ \rightarrow $-$, with $Y = -1$. The SM Higgs boson, h_0 , is a linear superposition
397 of the neutral components of these two doublets. The SUSY parts of the Higgs
398 multiplets, \tilde{H}_u and \tilde{H}_d , are each left-handed Weyl spinors. For generic spin-1/2
399 sparticles, we add the “-ino” suffix. We then call the partners of the two Higgs
400 collectively the *Higgsinos*.

²The last one should probably have bigger scare quotes.

Figure 3.1: Particles of the MSSM



401 Gauge supermultiplets

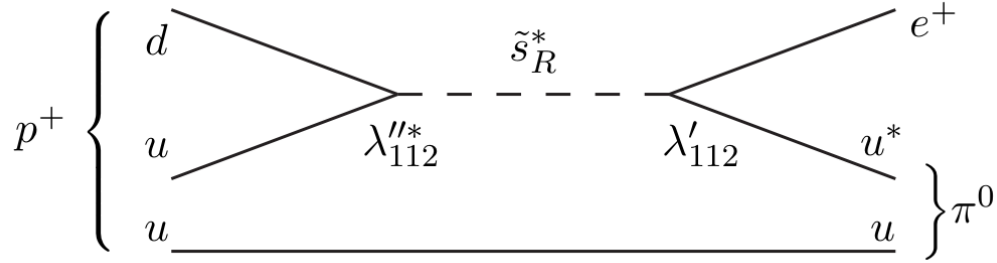
402 The superpartners of the gauge bosons must all be in gauge supermultiplets since
 403 they contain a spin-1 particle. Collectively, we refer to the superpartners of the
 404 gauge bosons as the gauginos.

405 The first gauge supermultiplet contains the gluon, and its superpartner, which is
 406 known as the *gluino*, denoted \tilde{g} . The gluon is of course the SM mediator of $SU(3)_C$;
 407 the gluino is also a colored particle, subject to $SU(3)_C$. From the SM before EWSB,
 408 we have the four gauge bosons of the electroweak symmetry group $SU(2)_L \otimes U(1)_Y$:
 409 $W^{1,2,3}$ and B^0 . The superpartners of these particles are thus the *winos* $\tilde{W}^{1,2,3}$ and
 410 *bino* \tilde{B}^0 , where each is placed in another gauge supermultiplet with its corresponding
 411 SM particle. After EWSB, without breaking supersymmetry, we would also have the
 412 zino \tilde{Z}^0 and photino $\tilde{\gamma}$.

413 The entire particle content of the MSSM can be seen in Fig.3.1.

414 At this point, it's important to take a step back. Where are these particles?
 415 As stated above, supersymmetric theories require that the masses and all quantum

Figure 3.2: This Feynmann diagram shows how proton decay is induced in the MSSM, if one does not impose R -parity.



416 numbers of the SM particle and its corresponding sparticle are the same. Of course,
 417 we have not observed a selectron, squark, or wino. The answer, as it often is, is that
 418 supersymmetry is *broken* by the vacuum state of nature [15].

419 R -parity

This section is a quick aside to the general story. R - *parity* refers to an additional discrete symmetry which is often imposed on supersymmetric models. For a given particle state, we define

$$R = (-1)^{3(B-L)+2s} \quad (3.9)$$

420 where B, L is the baryon (lepton) number and s is the spin. The imposition of
 421 this symmetry forbids certain terms from the MSSM Lagrangian that would violate
 422 baryon and/or lepton number. This is required in order to prevent proton decay, as
 423 shown in Fig.3.2³. .

424 In supersymmetric models, this is a \mathbb{Z}_2 symmetry, where SM particles have $R = 1$
 425 and sparticles have $R = -1$. We will take R - *parity* as part of the definition of
 426 the MSSM. We will discuss later the *drastic* consequences of this symmetry on SUSY
 427 phenomenology

³Proton decay can actually be prevented by allowing only one of the four potential R-parity violating terms to survive.

428 Soft supersymmetry breaking

The fundamental idea of *soft* supersymmetry breaking[15, 34, 35, 72, 73] is that we would like to break supersymmetry without reintroducing the quadratic divergences we discussed at the end of Chapter 2. We write the Lagrangian in a form :

$$\mathcal{L}_{\text{MSSM}} = \mathcal{L}_{\text{SUSY}} + \mathcal{L}_{\text{soft}} \quad (3.10)$$

429 In this sense, the symmetry breaking is “soft”, since we have separated out the
430 completely symmetric terms from those soft terms which will not allow the quadratic
431 divergences to the Higgs mass.

432 The explicitly allowed terms in the soft-breaking Lagrangian are [35].

- 433 • Mass terms for the scalar components of the chiral supermultipletss
- 434 • Mass terms for the Weyl spinor components of the gauge supermultipletss
- 435 • Trilinear couplings of scalar components of chiral supermultiplets

In particular, using the field content described above for the MSSM, the softly-broken portion of the MSSM Lagrangian can be written

$$\mathcal{L}_{\text{soft}} = -\frac{1}{2} \left(M_3 \tilde{g} \tilde{g} + M_2 \tilde{W} \tilde{W} + M_1 \tilde{B} \tilde{B} + c.c. \right) \quad (3.11)$$

$$- \left(\tilde{u} a_u \tilde{Q} H_u - \tilde{d} a_d \tilde{Q} H_d - \tilde{e} a_e \tilde{L} H_d + c.c. \right) \quad (3.12)$$

$$- \tilde{Q}^\dagger m_Q^2 \tilde{Q} - \tilde{L}^\dagger m_L^2 \tilde{L} - \tilde{u} m_u^2 \tilde{u}^\dagger - \tilde{d} m_d^2 \tilde{d}^\dagger - \tilde{e} m_e^2 \tilde{e}^\dagger \quad (3.13)$$

$$- m_{H_u}^2 H_u^* H_u - m_{H_d}^2 H_d^* H_d - (b H_u H_d + cc). \quad (3.14)$$

436 where we have introduced the following notations :

- 437 1. M_3, M_2, M_1 are the gluino, wino, and bino masses.
- 438 2. a_u, a_d, a_e are complex 3×3 matrices in family space.
- 439 3. $m_Q^2, m_u^2, m_d^2, m_L^2, m_e^2$ are hermitian 3×3 matrices in family space.

440 4. $m_{H_u}^2, m_{H_d}^2, b$ are the SUSY-breaking contributions to the Higgs potential.

441 We have written matrix terms without any sort of additional notational decoration
 442 to indicate their matrix nature, and we now show why. The first term 1 are
 443 straightforward; these are just the straightforward mass terms for these fields. There
 444 are strong constraints on the off-diagonal terms for the matrices of 2 [74, 75]; for
 445 simplicity, we will assume that each $a_i, i = u, d, e$ is proportional to the Yukawa
 446 coupling matrix : $a_i = A_{i0}y_i$. The matrices in ?? can be similarly constrained by
 447 experiments [68, 75–82] Finally, we assume that the elements 4 contributing to the
 448 Higgs potential as well as all of the 1 terms must be real, which limits the possible
 449 CP-violating interactions to those of the Standard Model. We thus only consider
 450 flavor-blind, CP-conserving interactions within the MSSM.

The important mixing for mass and gauge interaction eigenstates in the MSSM occurs within electroweak sector, in a process akin to EWSB in the Standard Model. The neutral portions of the Higgsinos doublets and the neutral gauginos ($\tilde{H}_u^0, \tilde{H}_d^0, \tilde{B}^0, \tilde{W}^0$ of the gauge interaction basis mix to form what are known as the *neutralinos* of mass basis :

$$M_{\tilde{\chi}} = \begin{pmatrix} M_1 & 0 & -c_\beta s_W m_Z & s_\beta s_W m_Z \\ 0 & M_2 & c_\beta c_W m_Z & -s_\beta c_W m_Z \\ -c_\beta s_W m_Z & c_\beta c_W m_Z & 0 & -\mu \\ s_\beta s_W m_Z & -s_\beta c_W m_Z & -\mu & 0 \end{pmatrix} \quad (3.15)$$

451 where $s(c)$ are the sine and cosine of angles related to EWSB, which introduced
 452 masses to the gauginos and higgsinos. Diagonalization of this matrix gives the four
 453 neutralino mass states, listed without loss of generality in order of increasing mass :
 454 $\chi_{1,2,3,4}^0$.

455 The neutralinos, especially the lightest neutralino $\tilde{\chi}_1^0$, are important ingredients
 456 in SUSY phenomenology.

457 The same process can be done for the electrically charged gauginos with
 458 the charged portions of the Higgsino doublets along with the charged winos
 459 $(\tilde{H}_u^+, \tilde{H}_d^+, \tilde{W}^+, \tilde{W}^-)$. This leads to the *charginos*, again in order of increasing mass
 460 : $\tilde{\chi}_{1,2}^\pm$.

461 3.3 Phenomenology

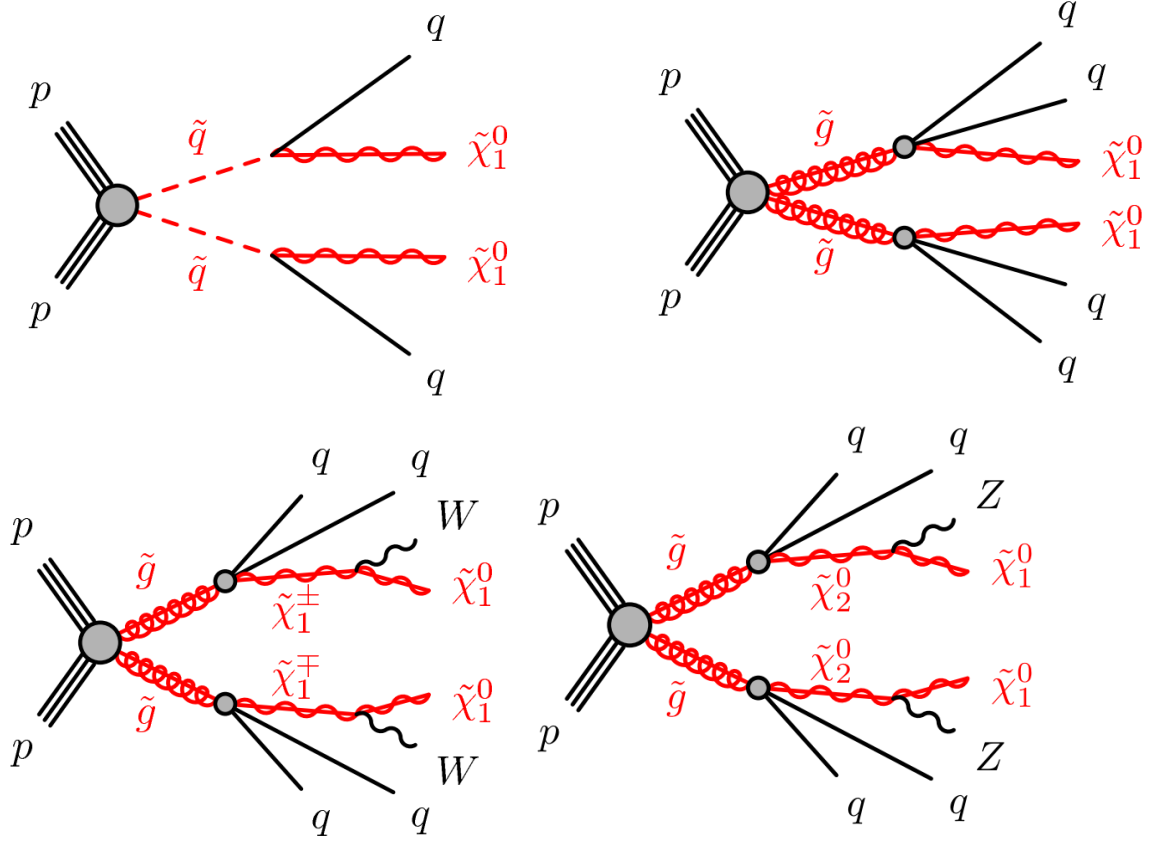
462 We are finally at the point where we can discuss the phenomenology of the MSSM,
 463 in particular as it manifests itself at the energy scales of the LHC.

464 As noted above in Sec.3.2, the assumption of R -parity has important conse-
 465 quences for MSSM phenomenology. The SM particles have $R = 1$, while the sparticles
 466 all have $R = -1$. Simply, this is the “charge” of supersymmetry. Since the particles of
 467 LHC collisions (pp) have total incoming $R = 1$, we must expect that all sparticles will
 468 be produced in *pairs*. An additional consequence of this symmetry is the fact that the
 469 lightest supersymmetric particle (LSP) is *stable*. Off each branch of the Feynmann
 470 diagram shown in Fig., we have $R = -1$, and this can only decay to another sparticle
 471 and a SM particle. Once we reach the lightest sparticle in the decay, it is absolutely
 472 stable. This leads to the common signature E_T^{miss} for a generic SUSY signal.

473 For this thesis, we will be presenting an inclusive search for squarks and gluinos
 474 with zero leptons in the final state. This is a very interesting decay channel⁴, due
 475 to the high cross-sections of $\tilde{g}\tilde{g}$ and $\tilde{q}\tilde{q}$ decays, as can be seen in Fig.?? [83]. This
 476 is a direct consequence of the fact that these are the colored particles of the MSSM.
 477 Since the sparticles interact with the gauge groups of the SM in the same way as their
 478 SM partners, the colored sparticles, the squarks and gluinos, are produced and decay
 479 as governed by the color group $SU(3)_C$ with the strong coupling g_s . The digluino
 480 production is particularly copious, due to color factor corresponding to the color octet

⁴Prior to Run1, probably the most *most* interesting SUSY decay channel.

Figure 3.3: SUSY signals considered in this thesis



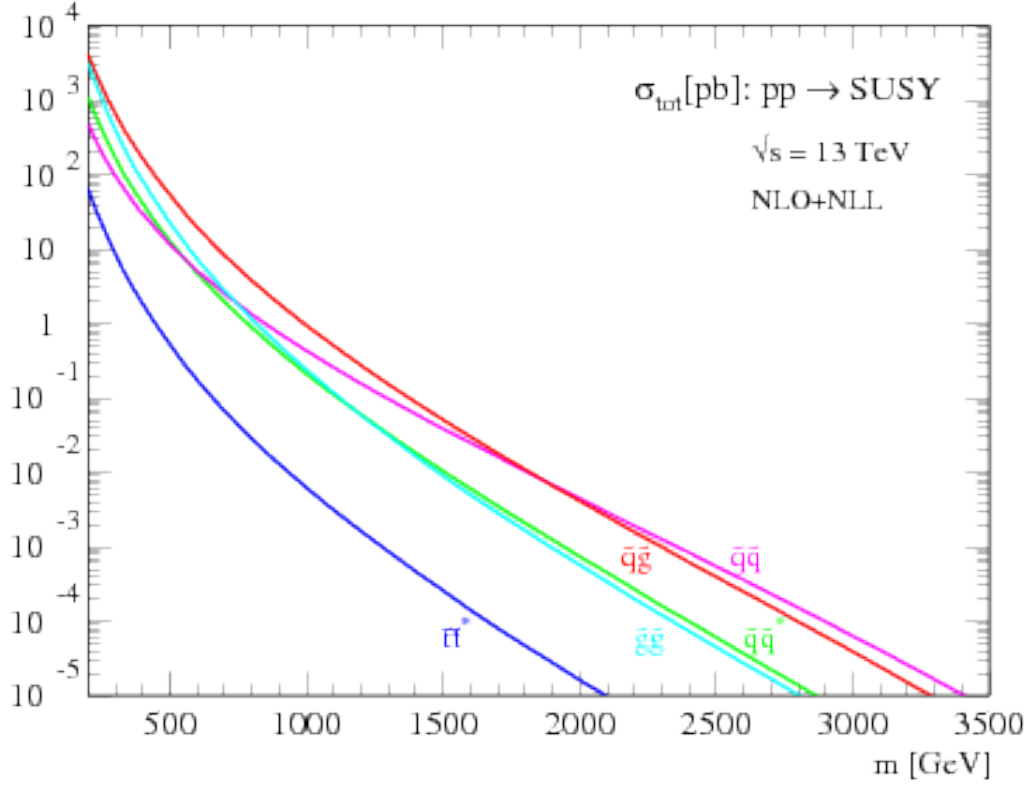
of $SU(3)C$.

In the case of disquark production, the most common decay mode of the squark in the MSSM is a decay directly to the LSP plus a single SM quark [15]. This means the basic search strategy of disquark production is two jets from the final state quarks, plus missing transverse energy for the LSPs. There are also cascade decays, the most common of which, and the only one considered in this thesis, is $\tilde{q} \rightarrow q\tilde{\chi}^\pm \rightarrow qW^\pm\chi^0$.

For digluino production, the most common decay is $\tilde{g} \rightarrow g\tilde{q}$, due to the large g_S coupling. The squark then decays as listed above. In this case, we generically search for four jets and missing transverse energy from the LSPs. We can also have the squark decay in association with a W^\pm or Z^0 ; in this thesis, we are interested in those cases where this vector boson goes hadronically.

In the context of experimental searches for SUSY, we often consider *simplified*

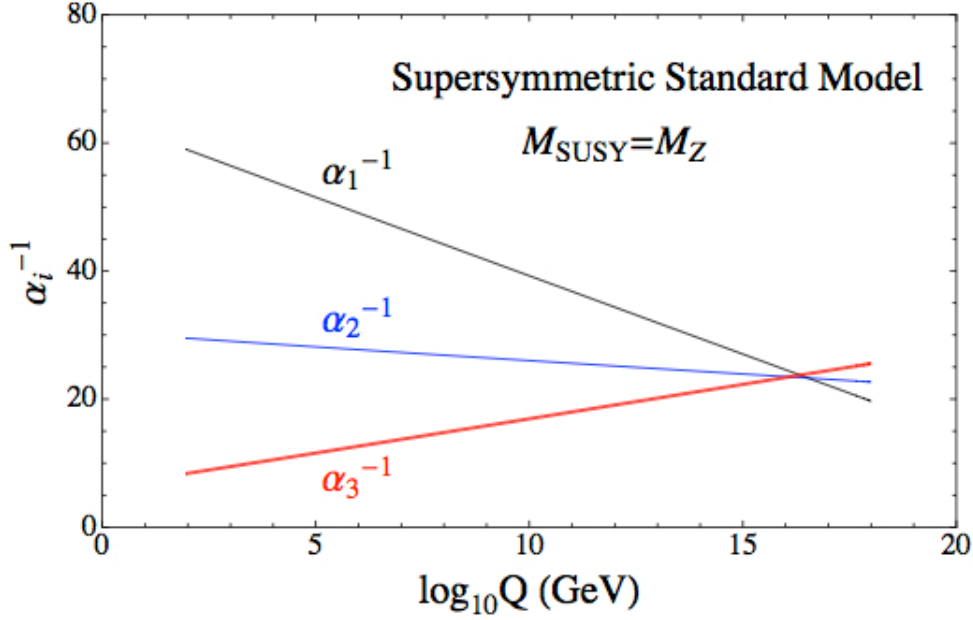
Figure 3.4: SUSY production cross-sections as a function of sparticle mass at $\sqrt{s} = 13$ TeV.



493 *models*. These models make certain assumptions which allow easy comparisons of
 494 results by theorists and rival experimentalists. In the context of this thesis, the
 495 simplified models will make assumptions about the branching ratios described in the
 496 preceding paragraphs. In particular, we will often choose a model where the decay of
 497 interest occurs with 100% branching ratio. This is entirely for ease of interpretation
 498 by other physicists⁵, but it is important to recognize that these are more a useful
 499 comparison tool, especially with limits, than a strict statement about the potential
 500 masses of sought-after beyond the Standard Model particle.

⁵In the author's opinion, this often leads to more confusion than comprehension. We will revisit the shortcomings of simplified models in the Conclusion to this thesis.

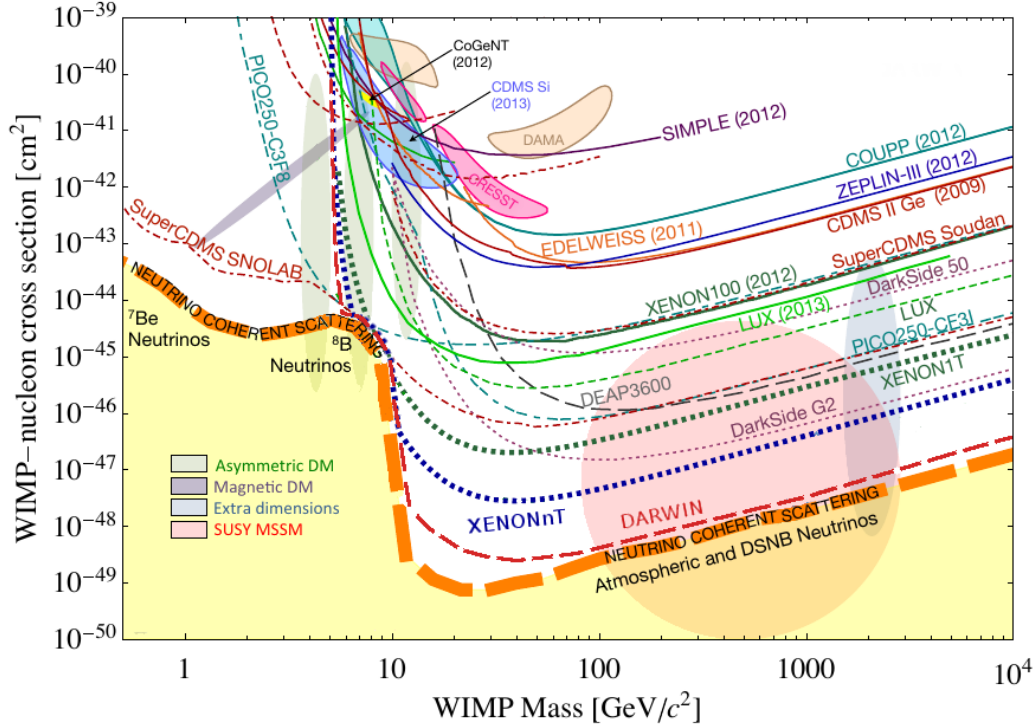
Figure 3.6: The running of Standard Model gauge couplings; compare to Fig.2.4. The MSSM gauge couplings nearly intersect at high energies.



516 Dark matter

517 As we discussed previously, the lack of any dark matter candidate in the Standard
518 Model naturally leads to beyond the Standard Model theories. In the Standard Model,
519 there is a natural dark matter candidate in the lightest supersymmetric particle[15]
520 The LSP would in dark matter experiments be called a *weakly-interacting massive*
521 *particle* (WIMP), which is a type of cold dark matter [22, 84]. These WIMPS would
522 only interact through the weak force and gravity, which is exactly as a model like the
523 MSSM predicts for the neutralino. In Fig.3.7, we can see the current WIMP exclusions
524 for a given mass. The range of allowed masses which have not been excluded for LSPs
525 and WIMPs have significant overlap. This provides additional motivation outside of
526 the context of theoretical details.

Figure 3.7: WIMP exclusions from direct dark matter detection experiments.



3.5 Conclusions

Supersymmetry is the most well-motivated theory for physics beyond the Standard Model. It provides a solution to the hierarchy problem, leads to gauge coupling unification, and provides a dark matter candidate consistent with galactic rotation curves. As noted in this chapter, due to the LSPs in the final state, most SUSY searches require a significant amount of missing transverse energy in combination with jets of high transverse momentum. However, there is some opportunity to do better than this, especially in final states where one has two weakly-interacting LSPs on opposite sides of some potentially complicated decay tree. We will see how this is done in Ch.??.

The Large Hadron Collider

539 The Large Hadron Collider (LHC) produces high-energy protons which are collided
540 at the center of multiple large experiments at CERN on the outskirts of Geneva,
541 Switzerland [85]. The LHC produces the highest energy collisions in the world,
542 with design center-of-mass energy of $\sqrt{s} = 14$ TeV, which allows the experiments
543 to investigate physics far beyond the reach of previous colliders. This chapter will
544 summarize the basics of accelerator physics, especially with regards to discovering
545 physics beyond the Standard Model. We will describe the CERN accelerator complex
546 and the LHC.

547 4.1 Basics of Accelerator Physics

548 This section follows closely the presentation of [86].

Simple particle accelerators simply rely on the acceleration of charged particles in a static electric field. Given a field of strength E , charge q , and mass m , this is simply

$$a = \frac{qE}{m}. \quad (4.1)$$

549 For a given particle with a given mass and charge, this is limited by the static electric
550 field which can be produced, which in turn is limited by electrical breakdown at high
551 voltages.

552 There are two complementary solutions to this issue. First, we use the *radio*
553 *frequency acceleration* technique. We call the devices used for this *RF cavities*. The

554 cavities produce a time-varied electric field, which oscillate such that the charged
 555 particles passing through it are accelerated towards the design energy of the RF
 556 cavity. This oscillation also induces the particles into *bunches*, since particles which
 557 are slightly off in energy from that induced by the RF cavity are accelerated towards
 558 the design energy.

Second, one bends the particles in a magnetic field, which allows them to pass through the same RF cavity over and over. This second process is often limited by *synchrotron radiation*, which describes the radiation produced when a charged particle is accelerated. The power radiated is

$$P \sim \frac{1}{r^2} \left(E/m \right)^4 \quad (4.2)$$

559 where r is the radius of curvature and E, m is the energy (mass) of the charged
 560 particle. Given an energy which can be produced by a given set of RF cavities (which
 561 is *not* limited by the mass of the particle), one then has two options to increase the
 562 actual collision energy : increase the radius of curvature or use a heavier particle.
 563 Practically speaking, the easiest options for particles in a collider are protons and
 564 electrons, since they are (obviously) copious in nature and do not decay¹. Given the
 565 dependence on mass, we can see why protons are used to reach the highest energies.
 566 The tradeoff for this is that protons are not point particles, and we thus we don't
 567 know the exact incoming four-vectors of the protons, as discussed in Ch.2.

The particle *beam* refers to the bunches all together An important property of a beam of a particular energy E , moving in uniform magnetic field B , containing particles of momentum p is the *beam rigidity* :

$$R \equiv rB = p/c. \quad (4.3)$$

568 The linear relation between r and p , or alternatively B and p have important
 569 consequences for LHC physics. For hadron colliders, this is the limiting factor on

¹Muon colliders are a really cool option at high energies, since the relativistic γ factor gives them a relatively long lifetime in the lab frame.

570 going to higher energy scales; one needs a proportionally larger magnetic field to
 571 keep the beam accelerating in a circle.

572 Besides the rigidity of the beam, the most important quantities to characterize
 573 a beam are known as the (normalized) *emittance* ϵ_N and the *betatron function* β .
 574 These quantities determine the transverse size σ of a relativistic beam $v \lesssim c$ beam :
 575 $\sigma^2 = \beta^* \epsilon_N / \gamma_{\text{rel}}$, where β^* is the value of the betatron function at the collision point
 576 and γ_{rel} is the Lorentz factor.

These quantities determine the *instaneous luminosity* L of a collider, which
 combined with the cross-section σ of a particular physics process, give the rate of
 this physics process :

$$R = L\sigma. \quad (4.4)$$

The instaneous luminosity L is given by :

$$L = \frac{f_{\text{rev}} N_b^2 F}{4\pi\sigma^2} = \frac{f_{\text{rev}} n N_b^2 \gamma_{\text{rel}} F}{4\pi\beta^* \epsilon_N}. \quad (4.5)$$

577 Here we have introduced the frequency of revolutions f_{rev} , the number of bunches n ,
 578 the number of protons per bunch N_b^2 , and a geometric factor F related to the crossing
 579 angle of the beams.

The *integrated luminosity* $\int L$ gives the total number of a particular physics
 process P , with cross-section σ_P .

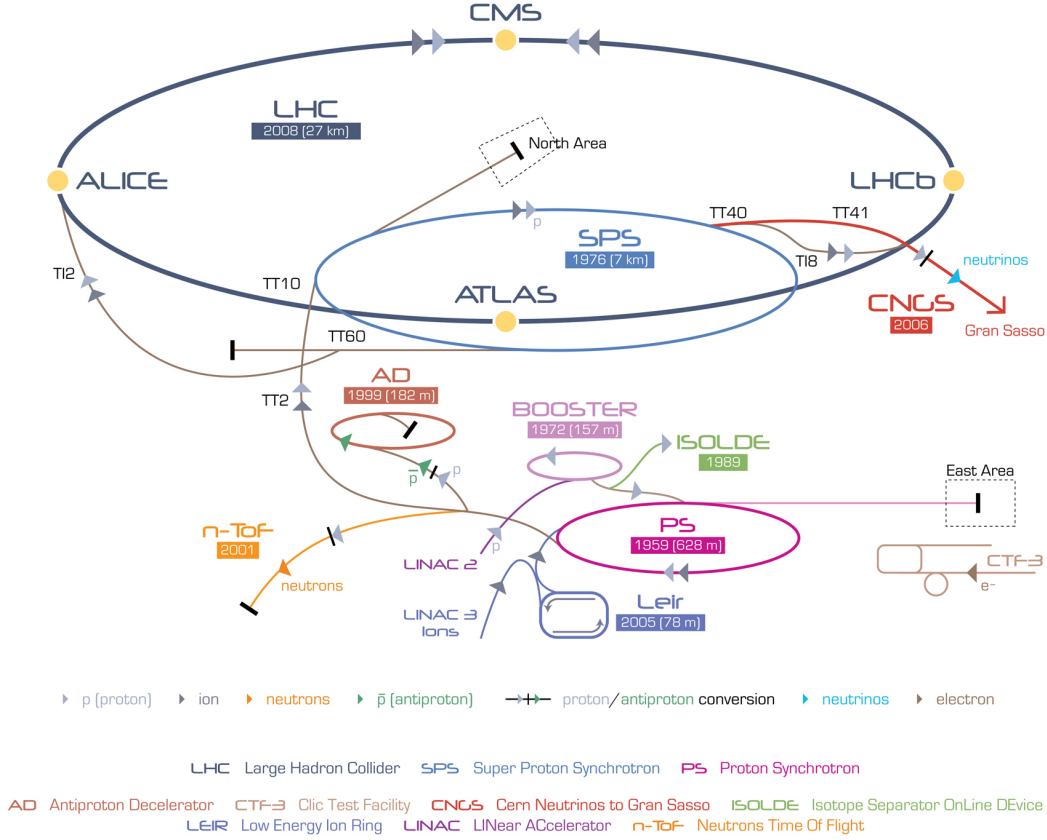
$$N_P = \sigma_P \int L. \quad (4.6)$$

580 Due to this simple relation, one can also quantify the “amount of data delivered” by
 581 a collider simply by $\int L$.

582 4.2 Accelerator Complex

583 The Large Hadron Collider is the last accelerator in a chain of accelerators which
 584 together form the CERN accelerator complex, which can be seen in [4.1](#). The protons

Figure 4.1: The CERN accelerator complex.



585 begin their journey to annihilation in a hydrogen source, where they are subsequently
 586 ionized. The first acceleration occurs in the Linac 2, a linear accelerator composed
 587 of RF cavities. The protons leave the Linac 2 at an energy of 50 MeV and enter
 588 the Proton Synchrotron Booster (PSB). The PSB contains four superimposed rings,
 589 which accelerate the protons to 1.4 GeV. The protons are then injected into the
 590 Proton Synchrotron (PS). This synchrotron increases the energy up to 25 GeV. After
 591 leaving the PS, the protons enter the Super Proton Synchrotron (SPS). This is the
 592 last step before entering the LHC ring, and the protons are accelerated to 450 GeV.
 593 From the SPS, the protons are injected into the beam pipes of the LHC. The process
 594 to fill the LHC rings with proton bunches from start to finish typically takes about
 595 four minutes.

596 4.3 Large Hadron Collider

The Large Hadron Collider is the final step in the CERN accelerator complex, and produces the collisions analyzed in this thesis. From the point of view of experimentalists on the general-purpose ATLAS and CMS experiments, the main goal of the LHC is to deliver collisions at the highest possible energy, with the highest possible instantaneous luminosity. The LHC was installed in the existing 27 km tunnel used by the Large Electron Positron (LEP) collider [87]. This allowed the existing accelerator complex at CERN, described in the previous section, to be used as the injection system to prepare the protons up to 450 GeV. Many aspects of the LHC design were decided by this very fact, and specified the options allowed to increase the energy or luminosity. In particular, the radius of the tunnel was already specified; from Eq.4.3, this implies the momentum (or energy) of the beam is entirely determined by the magnetic field. Given the 27 km circumference of the LEP tunnel, one can calculate the required magnetic field to reach the 7 TeV per proton design energy of the LHC :

$$r = C/2\pi = 4.3 \text{ km} \quad (4.7)$$

$$\rightarrow B = \frac{p}{rc} = 5 \text{ T} \quad (4.8)$$

597 In fact, the LHC consists of 8 528 m straight portions consisting of RF cavities, used
 598 to accelerate the particles, and 8 circular portions which bend the protons around the
 599 LHC ring. These circular portions actually have a slightly smaller radius of curvature
 600 $r = 2804 \text{ m}$, and we require $B = 8.33 \text{ T}$. To produce this large field, we need to use
 601 superconducting magnets, as discussed in the next section.

602 Magnets

603 There are many magnets used by the LHC machine, but the most important are the
 604 1232 dipole magnets; a schematic is shown in Fig.4.2 and a photograph is shown in

Figure 4.2: Schematic of an LHC dipole magnet.

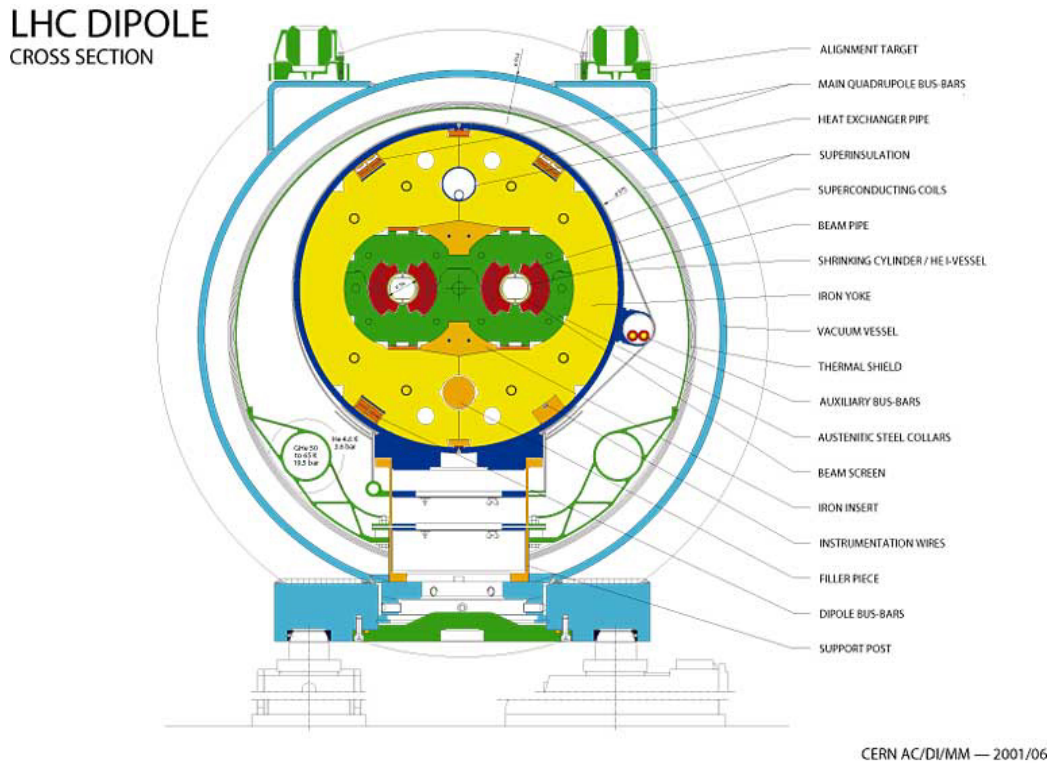


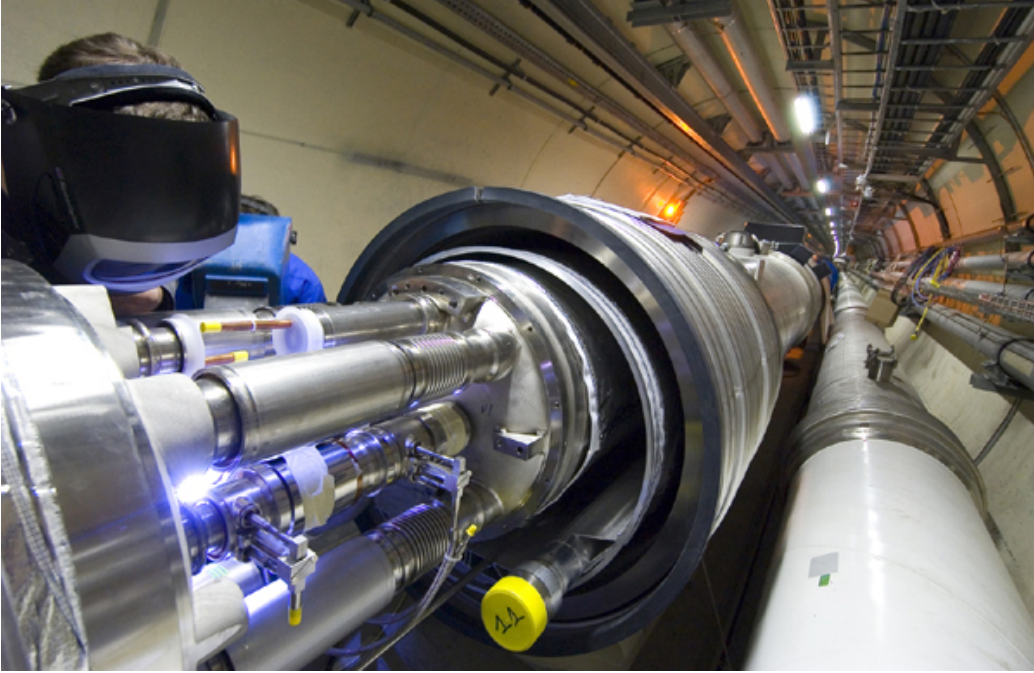
Fig.4.3.

The magnets are made of Niobium and Titanium. The maximum field strength is 10 T when cooled to 1.9 Kelvin. The magnets are cooled by superfluid helium, which is supplied by a large cryogenic system. Due to heating between the eight helium refrigerators and the beampipe, the helium is cooled in the refrigerators to 1.8 K.

A failure in the cooling system can cause what is known as a *quench*. If the temperature goes above the critical superconducting temperature, the metal loses its superconducting properties, which leads to a large resistance in the metal. This leads to rapid temperature increases, and can cause extensive damages if not controlled.

The dipole magnets are 16.5 meters long with a diameter of 0.57 meters. There are two individual beam pipes inside each magnet, which allows the dipoles to house the beams travelling in both directions around the LHC ring. They curve slightly, at an angle of 5.1 mrad, which carefully matches the curvature of the ring. The

Figure 4.3: Photograph of a technician connecting an LHC dipole magnet.



618 beampipes inside of the magnets are held in high vacuum, to avoid stray particles
619 interacting with the beam.

620 4.4 Dataset Delivered by the LHC

621 In this thesis, we analyze the data delivered by the LHC to ATLAS in the 2015 and
622 2016 datasets. The beam parameters relevant to this dataset are available in Table
623 [4.1](#).

624 The peak instantaneous luminosity delivered in 2015 (2016) was $L =$
625 $5.2(11) \text{ cm}^{-2} \text{ s}^{-1} \times 10^{33}$. One can note that the instantaneous luminosity delivered in
626 the 2016 dataset exceeds the design luminosity of the LHC. The total integrated
627 luminosity delivered was 13.3 fb^{-1} . In Figure [4.4](#), we display the integrated luminosity
628 as a function of day for 2015 and 2016.

Figure 4.4: Integrated Luminosity delivered by the LHC and collected by ATLAS in the 2015 and 2016 datasets.

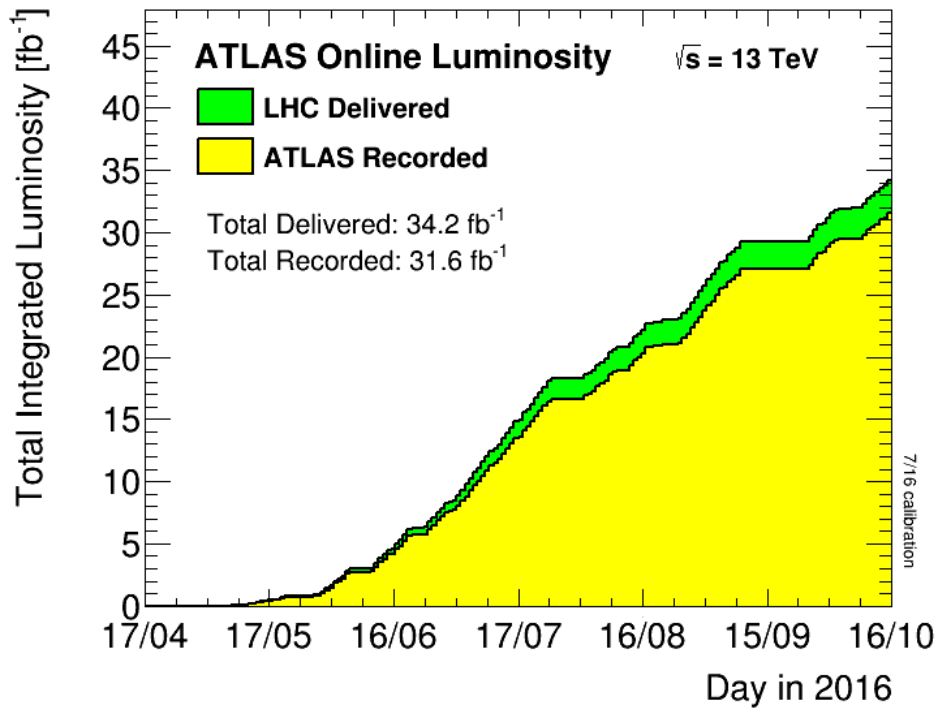
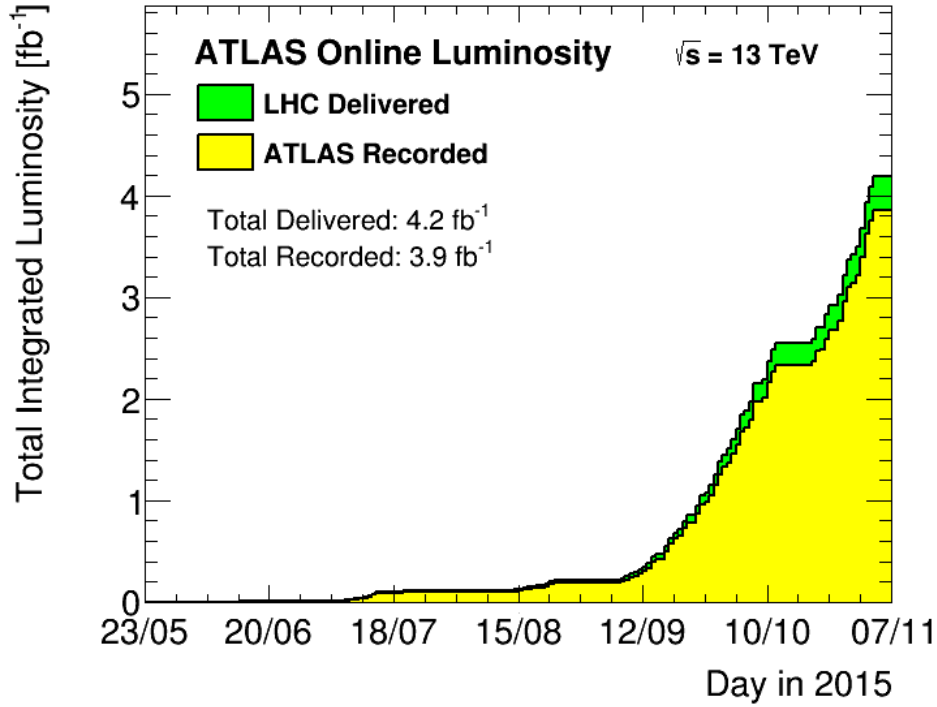
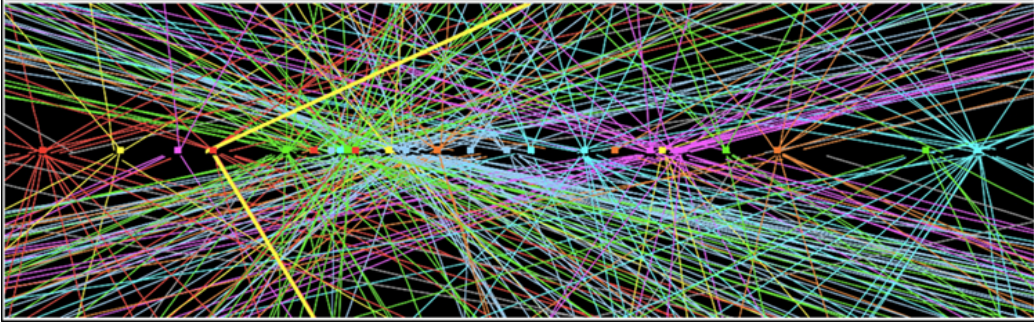


Table 4.1: Beam parameters of the Large Hadron Collider.

Parameter	Injection	Extraction
Energy (GeV)	450	7000
Rigidity (T-m)	3.8	23353
Bunch spacing (ns)	25	25
Design Luminosity ($\text{cm}^{-2}\text{s}^{-1} \times 10^{34}$)	-	1.0
Bunches per proton beam	2808	2808
Protons per bunch	1.15 e11	1.15 e11
Beam lifetime (hr)	-	10
Normalized Emittance ϵ_N (mm μrad)	3.3	3.75
Betatron function at collision point β^* (cm)	-	55

Figure 4.5: Simulated event with many pileup vertices.



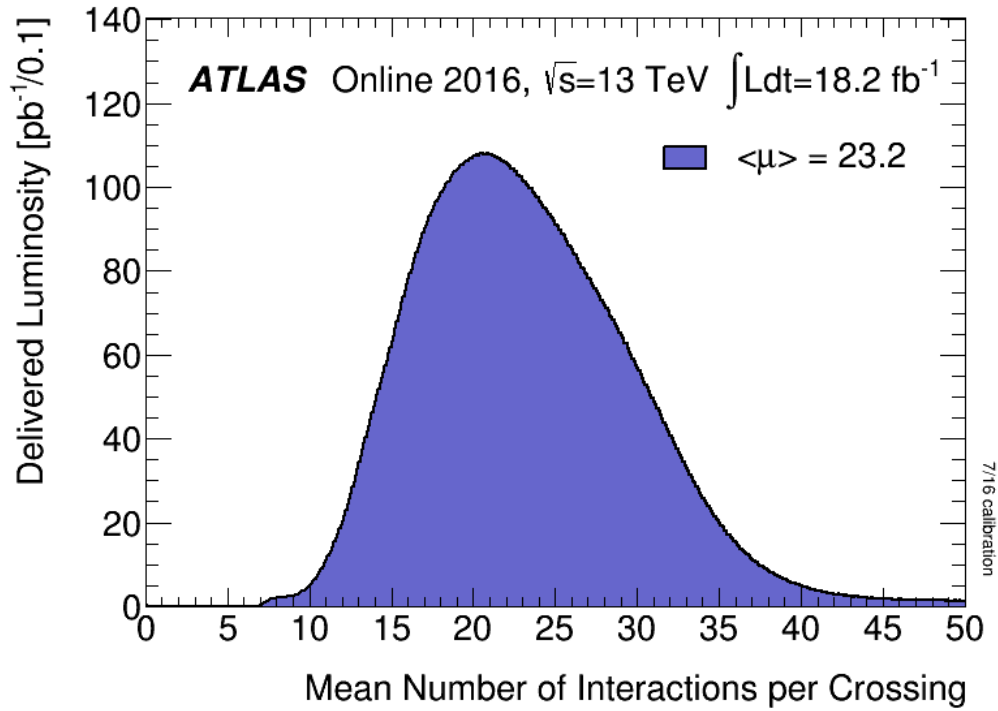
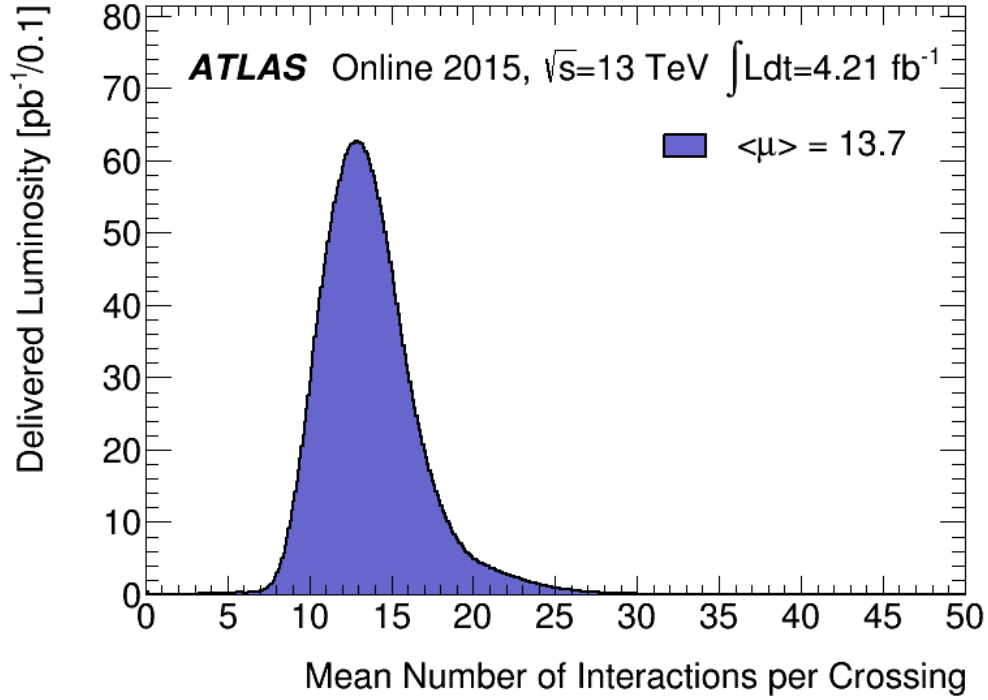
629 Pileup

630 *Pileup* is the term for the additional proton-proton interactions which occur during
631 each bunch crossing of the LHC. At the beginning of the LHC physics program, there
632 had not been a collider which averaged more than a single interaction per bunch
633 crossing. In the LHC, each bunch crossing (or *event*) generally contains multiple
634 proton-proton interactions. An simulated event with many *vertices* can be seen in
635 Fig.4.5 The so-called *primary vertex* (or *hard scatter vertex*) refers to the vertex which
636 has the highest Σp_T^2 ; this summation occurs over the *tracks* in the detector, which
637 we will describe later. We then distinguish between *in-time* pileup and *out-of-time*
638 pileup. In-time pileup refers to the additional proton-proton interactions which occur
639 in the event. Out-of-time pileup refers to effects related to proton-proton interactions
640 previous bunch crossings.

641 We quantify in-time pileup by the number of “primary”² vertices in a particular
642 event. To quantify the out-of-time pileup, we use the average number of interactions
643 per bunch crossing $\langle \mu \rangle$ over some human-scale time. In Figure 4.6, we show the
644 distribution of μ for the dataset used in this thesis.

²The primary vertex is as defined above, but we unfortunately use the same name here.

Figure 4.6: Mean number of interactions per bunch crossing in the 2015 and 2016 datasets.



645

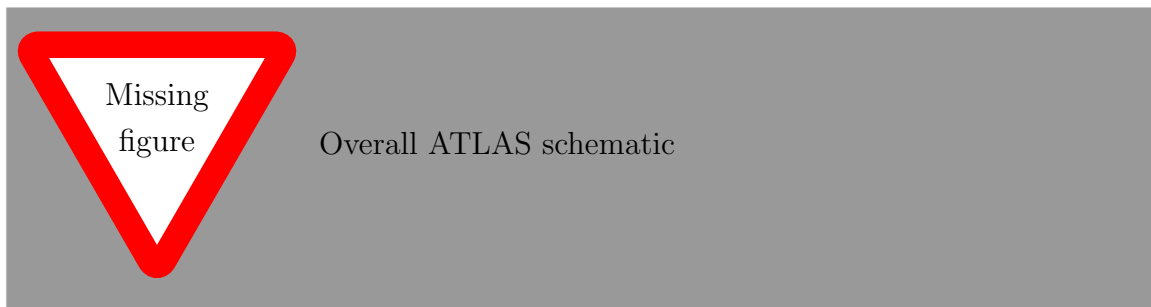
Chapter 5

646

The ATLAS detector

647 Here you can write some introductory remarks about your chapter. I like to give each
648 sentence its own line.

649 When you need a new paragraph, just skip an extra line.



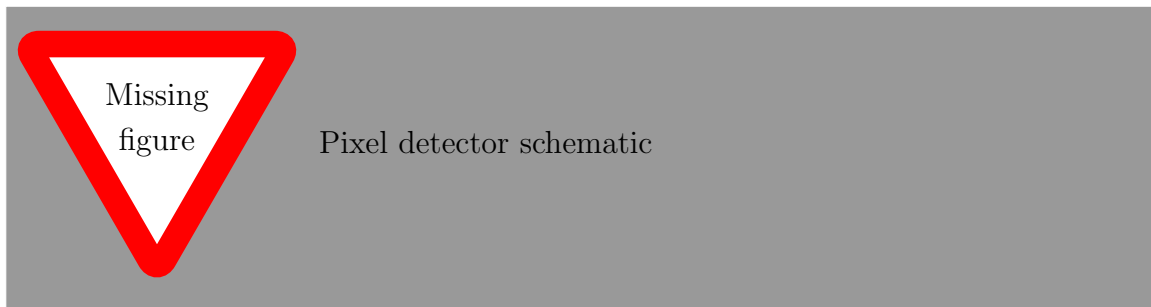
650

651

652 **5.1 Inner Detector**

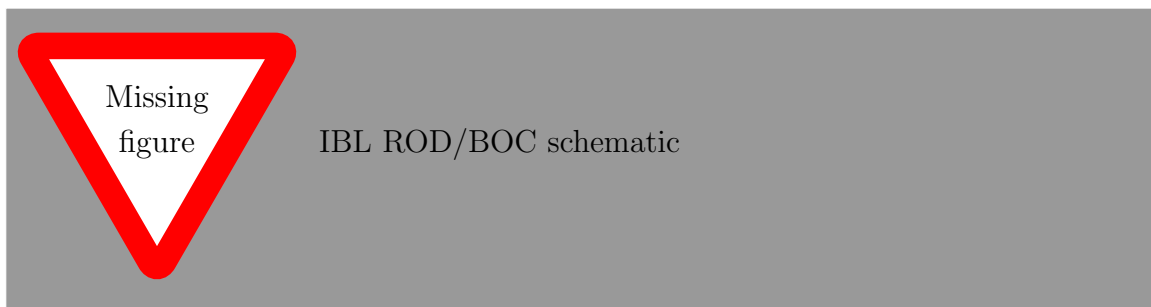
653 By using the asterisk to start a new section, I keep the section from appearing in the
654 table of contents. If you want your sections to be numbered and to appear in the
655 table of contents, remove the asterisk.

656 **Pixel Detector**

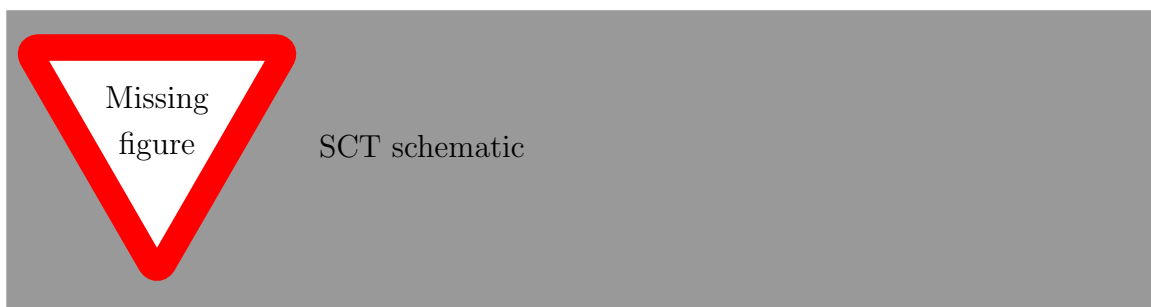


659 **Insertable B-Layer**

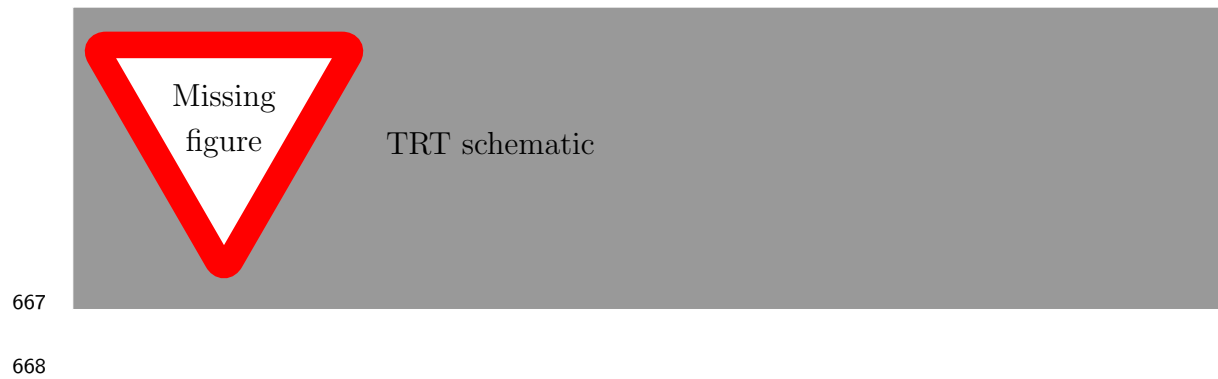
660 Qualification task, so add a bit more.



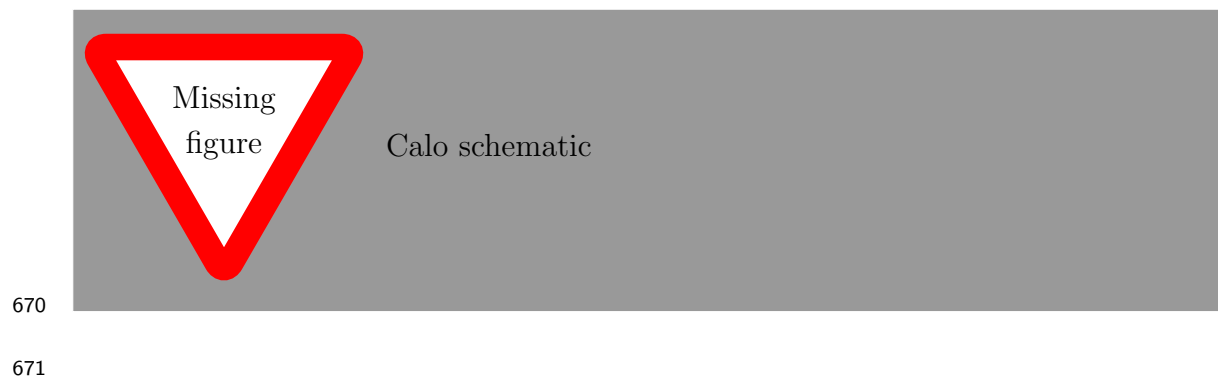
663 **Semiconductor Tracker**



666 **Transition Radiation Tracker**



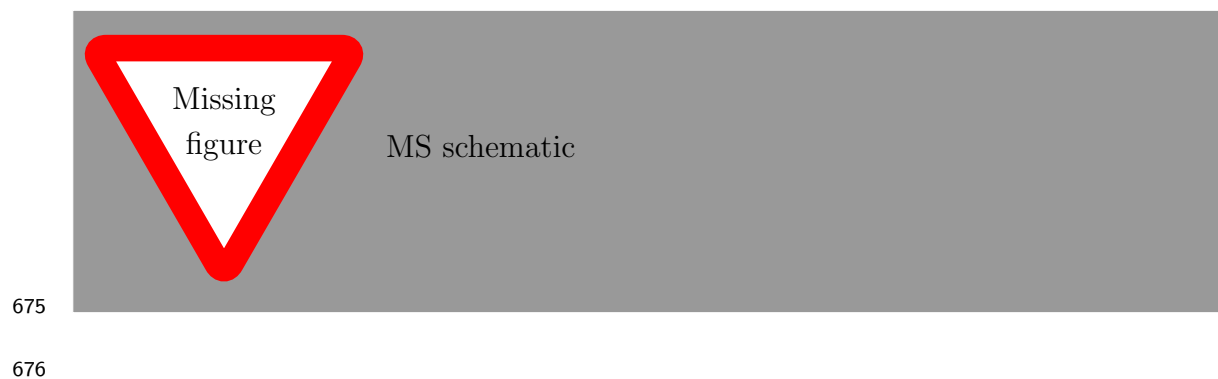
669 **5.2 Calorimeter**



672 **Electromagnetic Calorimeter**

673 **Hadronic Calorimeter**

674 **5.3 Muon Spectrometer**



The Recursive Jigsaw Technique

679 Here you can write some introductory remarks about your chapter. I like to give each
680 sentence its own line.

681 When you need a new paragraph, just skip an extra line.

682 **6.1 Razor variables**

683 By using the asterisk to start a new section, I keep the section from appearing in the
684 table of contents. If you want your sections to be numbered and to appear in the
685 table of contents, remove the asterisk.

686 **6.2 SuperRazor variables**

687 **6.3 The Recursive Jigsaw Technique**

688 **6.4 Variables used in the search for zero lepton**

689 **SUSY**

Title of Chapter 1

692

Chapter 8

693

Title of Chapter 1

694 Here you can write some introductory remarks about your chapter. I like to give each
695 sentence its own line.

696 When you need a new paragraph, just skip an extra line.

697 **8.1 Object reconstruction**

698 **Photons, Muons, and Electrons**

699 **Jets**

700 **Missing transverse momentum**

701 Probably longer, show some plots from the PUB note that we worked on

702 **8.2 Signal regions**

703 **Gluino signal regions**

704 **Squark signal regions**

705 **Compressed signal regions**

706 **8.3 Background estimation**

707 **Z $\nu\nu$**

708 **W $e\nu$**

709 **$t\bar{t}$**

710

Chapter 9

711

Title of Chapter 1

712 Here you can write some introductory remarks about your chapter. I like to give each
713 sentence its own line.

714 When you need a new paragraph, just skip an extra line.

715 **9.1 Statistical Analysis**

716 maybe to be moved to an appendix

717 **9.2 Signal Region distributions**

718 **9.3 Pull Plots**

719 **9.4 Systematic Uncertainties**

720 **9.5 Exclusion plots**

721

Conclusion

722 Here you can write some introductory remarks about your chapter. I like to give each
723 sentence its own line.

724 When you need a new paragraph, just skip an extra line.

725 **9.6 New Section**

726 By using the asterisk to start a new section, I keep the section from appearing in the
727 table of contents. If you want your sections to be numbered and to appear in the
728 table of contents, remove the asterisk.

Bibliography

- [1] O. Perdereau, *Planck 2015 cosmological results*,
AIP Conf. Proc. **1743** (2016) p. 050014.
- [2] N. Aghanim et al.,
*Planck 2016 intermediate results. LI. Features in the cosmic microwave
background temperature power spectrum and shifts in cosmological parameters*
(2016), arXiv: [1608.02487 \[astro-ph.CO\]](#).
- [3] J. S. Schwinger,
On Quantum electrodynamics and the magnetic moment of the electron,
Phys. Rev. **73** (1948) p. 416.
- [4] S. Laporta and E. Remiddi,
The Analytical value of the electron ($g-2$) at order α^3 in QED,
Phys. Lett. **B379** (1996) p. 283, arXiv: [hep-ph/9602417 \[hep-ph\]](#).
- [5] S. Schael et al., *Precision electroweak measurements on the Z resonance*,
Phys. Rept. **427** (2006) p. 257, arXiv: [hep-ex/0509008 \[hep-ex\]](#).
- [6] S. L. Glashow, *Partial Symmetries of Weak Interactions*,
Nucl. Phys. **22** (1961) p. 579.
- [7] S. Weinberg, *A Model of Leptons*, Phys. Rev. Lett. **19** (1967) p. 1264.
- [8] A. Salam, *Weak and Electromagnetic Interactions*,
Conf. Proc. **C680519** (1968) p. 367.
- [9] M. Gell-Mann, *A Schematic Model of Baryons and Mesons*,
Phys. Lett. **8** (1964) p. 214.
- [10] G. Zweig, “An SU(3) model for strong interaction symmetry and its breaking.
Version 2,” *DEVELOPMENTS IN THE QUARK THEORY OF HADRONS*.
VOL. 1. 1964 - 1978, ed. by D. Lichtenberg and S. P. Rosen, 1964 p. 22,
URL: <http://inspirehep.net/record/4674/files/cern-th-412.pdf>.

- 755 [11] S. Weinberg, *Implications of Dynamical Symmetry Breaking*,
756 [Phys. Rev. **D13** \(1976\) p. 974.](#)
- 757 [12] S. Weinberg, *Implications of Dynamical Symmetry Breaking: An Addendum*,
758 [Phys. Rev. **D19** \(1979\) p. 1277.](#)
- 759 [13] E. Gildener, *Gauge Symmetry Hierarchies*, [Phys. Rev. **D14** \(1976\) p. 1667.](#)
- 760 [14] L. Susskind,
761 *Dynamics of Spontaneous Symmetry Breaking in the Weinberg-Salam Theory*,
762 [Phys. Rev. **D20** \(1979\) p. 2619.](#)
- 763 [15] S. P. Martin, “A Supersymmetry Primer,” 1997,
764 eprint: [arXiv:hep-ph/9709356](#).
- 765 [16] V. C. Rubin and W. K. Ford Jr., *Rotation of the Andromeda Nebula from a*
766 *Spectroscopic Survey of Emission Regions*, [Astrophys. J. **159** \(1970\) p. 379.](#)
- 767 [17] M. S. Roberts and R. N. Whitehurst,
768 “*The rotation curve and geometry of M31 at large galactocentric distances*,
769 *Astrophys. J.* **201** (1970) p. 327.
- 770 [18] V. C. Rubin, N. Thonnard, and W. K. Ford Jr.,
771 *Rotational properties of 21 SC galaxies with a large range of luminosities and*
772 *radii, from NGC 4605 /R = 4kpc/ to UGC 2885 /R = 122 kpc/*,
773 [Astrophys. J. **238** \(1980\) p. 471.](#)
- 774 [19] V. C. Rubin et al., *Rotation velocities of 16 SA galaxies and a comparison of*
775 *Sa, Sb, and SC rotation properties*, [Astrophys. J. **289** \(1985\) p. 81.](#)
- 776 [20] A. Bosma,
777 *21-cm line studies of spiral galaxies. 2. The distribution and kinematics of*
778 *neutral hydrogen in spiral galaxies of various morphological types.*,
779 [Astron. J. **86** \(1981\) p. 1825.](#)
- 780 [21] M. Persic, P. Salucci, and F. Stel, *The Universal rotation curve of spiral*
781 *galaxies: 1. The Dark matter connection*,
782 [Mon. Not. Roy. Astron. Soc. **281** \(1996\) p. 27,](#)
783 [arXiv: astro-ph/9506004 \[astro-ph\].](#)
- 784 [22] M. Lisanti, “Lectures on Dark Matter Physics,” 2016,
785 eprint: [arXiv:1603.03797](#).
- 786 [23] H. Miyazawa, *Baryon Number Changing Currents*,
787 [Prog. Theor. Phys. **36** \(1966\) p. 1266.](#)

- [24] J.-L. Gervais and B. Sakita, *Generalizations of dual models*,
Nucl. Phys. **B34** (1971) p. 477.
- [25] J.-L. Gervais and B. Sakita,
Field Theory Interpretation of Supergauges in Dual Models,
Nucl. Phys. **B34** (1971) p. 632.
- [26] Yu. A. Golfand and E. P. Likhtman, *Extension of the Algebra of Poincare
Group Generators and Violation of p Invariance*,
JETP Lett. **13** (1971) p. 323, [Pisma Zh. Eksp. Teor. Fiz.13,452(1971)].
- [27] A. Neveu and J. H. Schwarz, *Factorizable dual model of pions*,
Nucl. Phys. **B31** (1971) p. 86.
- [28] A. Neveu and J. H. Schwarz, *Quark Model of Dual Pions*,
Phys. Rev. **D4** (1971) p. 1109.
- [29] D. V. Volkov and V. P. Akulov, *Is the Neutrino a Goldstone Particle?*
Phys. Lett. **B46** (1973) p. 109.
- [30] J. Wess and B. Zumino,
A Lagrangian Model Invariant Under Supergauge Transformations,
Phys. Lett. **B49** (1974) p. 52.
- [31] A. Salam and J. A. Strathdee, *Supersymmetry and Nonabelian Gauges*,
Phys. Lett. **B51** (1974) p. 353.
- [32] S. Ferrara, J. Wess, and B. Zumino, *Supergauge Multiplets and Superfields*,
Phys. Lett. **B51** (1974) p. 239.
- [33] J. Wess and B. Zumino, *Supergauge Transformations in Four-Dimensions*,
Nucl. Phys. **B70** (1974) p. 39.
- [34] J. D. Lykken, “Introduction to supersymmetry,” *Fields, strings and duality.
Proceedings, Summer School, Theoretical Advanced Study Institute in
Elementary Particle Physics, TASI’96, Boulder, USA, June 2-28, 1996*, 1996
p. 85, arXiv: [hep-th/9612114](https://arxiv.org/abs/hep-th/9612114) [hep-th],
URL: http://lss.fnal.gov/cgi-bin/find_paper.pl?pub-96-445-T.
- [35] A. Kobakhidze, “Intro to SUSY,” 2016, URL:
<https://indico.cern.ch/event/443176/page/5225-pre-susy-programme>.
- [36] G. R. Farrar and P. Fayet, *Phenomenology of the Production, Decay, and
Detection of New Hadronic States Associated with Supersymmetry*,
Phys. Lett. **B76** (1978) p. 575.

- [37] ATLAS Collaboration,
Search for the electroweak production of supersymmetric particles in
 $\sqrt{s} = 8 \text{ TeV}$ *pp collisions with the ATLAS detector*,
Phys. Rev. D **93** (2016) p. 052002, arXiv: [1509.07152 \[hep-ex\]](#).
- [38] ATLAS Collaboration, *Summary of the searches for squarks and gluinos using*
 $\sqrt{s} = 8 \text{ TeV}$ *pp collisions with the ATLAS experiment at the LHC*,
JHEP **10** (2015) p. 054, arXiv: [1507.05525 \[hep-ex\]](#).
- [39] ATLAS Collaboration, *ATLAS Run 1 searches for direct pair production of*
third-generation squarks at the Large Hadron Collider,
Eur. Phys. J. C **75** (2015) p. 510, arXiv: [1506.08616 \[hep-ex\]](#).
- [40] CMS Collaboration,
Search for supersymmetry with razor variables in pp collisions at $\sqrt{s} = 7 \text{ TeV}$,
Phys. Rev. D **90** (2014) p. 112001, arXiv: [1405.3961 \[hep-ex\]](#).
- [41] CMS Collaboration, *Inclusive search for supersymmetry using razor variables*
in pp collisions at $\sqrt{s} = 7 \text{ TeV}$, *Phys. Rev. Lett.* **111** (2013) p. 081802,
arXiv: [1212.6961 \[hep-ex\]](#).
- [42] CMS Collaboration, *Search for Supersymmetry in pp Collisions at 7 TeV in*
Events with Jets and Missing Transverse Energy,
Phys. Lett. B **698** (2011) p. 196, arXiv: [1101.1628 \[hep-ex\]](#).
- [43] CMS Collaboration, *Search for Supersymmetry at the LHC in Events with*
Jets and Missing Transverse Energy, *Phys. Rev. Lett.* **107** (2011) p. 221804,
arXiv: [1109.2352 \[hep-ex\]](#).
- [44] CMS Collaboration, *Search for supersymmetry in hadronic final states using*
 M_{T2} *in pp collisions at $\sqrt{s} = 7 \text{ TeV}$* , *JHEP* **10** (2012) p. 018,
arXiv: [1207.1798 \[hep-ex\]](#).
- [45] CMS Collaboration, *Searches for supersymmetry using the M_{T2} variable in*
hadronic events produced in pp collisions at 8 TeV, *JHEP* **05** (2015) p. 078,
arXiv: [1502.04358 \[hep-ex\]](#).
- [46] CMS Collaboration, *Search for new physics with the M_{T2} variable in all-jets*
final states produced in pp collisions at $\sqrt{s} = 13 \text{ TeV}$ (2016),
arXiv: [1603.04053 \[hep-ex\]](#).
- [47] ATLAS Collaboration, *Multi-channel search for squarks and gluinos in*
 $\sqrt{s} = 7 \text{ TeV}$ *pp collisions with the ATLAS detector at the LHC*,
Eur. Phys. J. C **73** (2013) p. 2362, arXiv: [1212.6149 \[hep-ex\]](#).

- [48] Y. Grossman, “Introduction to the SM,” 2016, URL: <https://indico.fnal.gov/sessionDisplay.py?sessionId=3&confId=11505#20160811>.
- [49] ().
- [50] P. W. Higgs, *Broken Symmetries and the Masses of Gauge Bosons*, *Phys. Rev. Lett.* **13** (1964) p. 508.
- [51] ATLAS Collaboration, *Observation of a new particle in the search for the Standard Model Higgs boson with the ATLAS detector at the LHC*, *Phys. Lett. B* **716** (2012) p. 1, arXiv: [1207.7214 \[hep-ex\]](#).
- [52] CMS Collaboration, *Observation of a new boson at a mass of 125 GeV with the CMS experiment at the LHC*, *Phys. Lett. B* **716** (2012) p. 30, arXiv: [1207.7235 \[hep-ex\]](#).
- [53] A. Chodos et al., *A New Extended Model of Hadrons*, *Phys. Rev.* **D9** (1974) p. 3471.
- [54] A. Chodos et al., *Baryon Structure in the Bag Theory*, *Phys. Rev.* **D10** (1974) p. 2599.
- [55] J. C. Collins, D. E. Soper, and G. F. Sterman, *Factorization of Hard Processes in QCD*, *Adv. Ser. Direct. High Energy Phys.* **5** (1989) p. 1, arXiv: [hep-ph/0409313 \[hep-ph\]](#).
- [56] K. A. Olive et al., *Review of Particle Physics*, *Chin. Phys.* **C38** (2014) p. 090001.
- [57] N. Cabibbo, *Unitary Symmetry and Leptonic Decays*, *Phys. Rev. Lett.* **10** (1963) p. 531, [648(1963)].
- [58] M. Kobayashi and T. Maskawa, *CP Violation in the Renormalizable Theory of Weak Interaction*, *Prog. Theor. Phys.* **49** (1973) p. 652.
- [59] W. F. L. Hollik, *Radiative Corrections in the Standard Model and their Role for Precision Tests of the Electroweak Theory*, *Fortsch. Phys.* **38** (1990) p. 165.
- [60] D. Yu. Bardin et al., *ELECTROWEAK RADIATIVE CORRECTIONS TO DEEP INELASTIC SCATTERING AT HERA! CHARGED CURRENT SCATTERING*, *Z. Phys.* **C44** (1989) p. 149.

- 888 [61] D. C. Kennedy et al., *Electroweak Cross-Sections and Asymmetries at the Z0*,
889 [Nucl. Phys. **B321** \(1989\) p. 83.](#)
- 890 [62] A. Sirlin, *Radiative Corrections in the $SU(2)_L \times U(1)$ Theory: A Simple*
891 *Renormalization Framework*, [Phys. Rev. **D22** \(1980\) p. 971.](#)
- 892 [63] S. Fanchiotti, B. A. Kniehl, and A. Sirlin,
893 *Incorporation of QCD effects in basic corrections of the electroweak theory*,
894 [Phys. Rev. **D48** \(1993\) p. 307](#), arXiv: [hep-ph/9212285 \[hep-ph\]](#).
- 895 [64] C. Quigg, “Cosmic Neutrinos,” *Proceedings, 35th SLAC Summer Institute on*
896 *Particle Physics: Dark matter: From the cosmos to the Laboratory (SSI 2007):*
897 *Menlo Park, California, July 30- August 10, 2007*, 2008,
898 arXiv: [0802.0013 \[hep-ph\]](#),
899 URL: http://lss.fnal.gov/cgi-bin/find_paper.pl?conf-07-417.
- 900 [65] S. R. Coleman and J. Mandula, *All Possible Symmetries of the S Matrix*,
901 [Phys. Rev. **159** \(1967\) p. 1251.](#)
- 902 [66] R. Haag, J. T. Lopuszanski, and M. Sohnius,
903 *All Possible Generators of Supersymmetries of the s Matrix*,
904 [Nucl. Phys. **B88** \(1975\) p. 257.](#)
- 905 [67] A. Salam and J. A. Strathdee, *On Superfields and Fermi-Bose Symmetry*,
906 [Phys. Rev. **D11** \(1975\) p. 1521.](#)
- 907 [68] S. Dimopoulos and H. Georgi, *Softly Broken Supersymmetry and $SU(5)$* ,
908 [Nucl. Phys. **B193** \(1981\) p. 150.](#)
- 909 [69] S. Dimopoulos, S. Raby, and F. Wilczek,
910 *Supersymmetry and the Scale of Unification*, [Phys. Rev. **D24** \(1981\) p. 1681.](#)
- 911 [70] L. E. Ibanez and G. G. Ross,
912 *Low-Energy Predictions in Supersymmetric Grand Unified Theories*,
913 [Phys. Lett. **B105** \(1981\) p. 439.](#)
- 914 [71] W. J. Marciano and G. Senjanovic,
915 *Predictions of Supersymmetric Grand Unified Theories*,
916 [Phys. Rev. **D25** \(1982\) p. 3092.](#)
- 917 [72] L. Girardello and M. T. Grisaru, *Soft Breaking of Supersymmetry*,
918 [Nucl. Phys. **B194** \(1982\) p. 65.](#)

- 919 [73] D. J. H. Chung et al.,
 920 *The Soft supersymmetry breaking Lagrangian: Theory and applications*,
 921 *Phys. Rept.* **407** (2005) p. 1, arXiv: [hep-ph/0312378](#) [[hep-ph](#)].
- 922 [74] J. Hisano et al., *Lepton flavor violation in the supersymmetric standard model*
 923 *with seesaw induced neutrino masses*, *Phys. Lett.* **B357** (1995) p. 579,
 924 arXiv: [hep-ph/9501407](#) [[hep-ph](#)].
- 925 [75] F. Gabbiani et al., *A Complete analysis of FCNC and CP constraints in*
 926 *general SUSY extensions of the standard model*,
 927 *Nucl. Phys.* **B477** (1996) p. 321, arXiv: [hep-ph/9604387](#) [[hep-ph](#)].
- 928 [76] F. Gabbiani and A. Masiero, *FCNC in Generalized Supersymmetric Theories*,
 929 *Nucl. Phys.* **B322** (1989) p. 235.
- 930 [77] J. S. Hagelin, S. Kelley, and T. Tanaka, *Supersymmetric flavor changing*
 931 *neutral currents: Exact amplitudes and phenomenological analysis*,
 932 *Nucl. Phys.* **B415** (1994) p. 293.
- 933 [78] J. S. Hagelin, S. Kelley, and V. Ziegler, *Using gauge coupling unification and*
 934 *proton decay to test minimal supersymmetric SU(5)*,
 935 *Phys. Lett.* **B342** (1995) p. 145, arXiv: [hep-ph/9406366](#) [[hep-ph](#)].
- 936 [79] D. Choudhury et al.,
 937 *Constraints on nonuniversal soft terms from flavor changing neutral currents*,
 938 *Phys. Lett.* **B342** (1995) p. 180, arXiv: [hep-ph/9408275](#) [[hep-ph](#)].
- 939 [80] R. Barbieri and L. J. Hall, *Signals for supersymmetric unification*,
 940 *Phys. Lett.* **B338** (1994) p. 212, arXiv: [hep-ph/9408406](#) [[hep-ph](#)].
- 941 [81] B. de Carlos, J. A. Casas, and J. M. Moreno,
 942 *Constraints on supersymmetric theories from $\mu \rightarrow e \gamma$* ,
 943 *Phys. Rev.* **D53** (1996) p. 6398, arXiv: [hep-ph/9507377](#) [[hep-ph](#)].
- 944 [82] J. A. Casas and S. Dimopoulos,
 945 *Stability bounds on flavor violating trilinear soft terms in the MSSM*,
 946 *Phys. Lett.* **B387** (1996) p. 107, arXiv: [hep-ph/9606237](#) [[hep-ph](#)].
- 947 [83] C. Borschensky et al., *Squark and gluino production cross sections in pp*
 948 *collisions at $\sqrt{s} = 13, 14, 33$ and 100 TeV*, *Eur. Phys. J.* **C74** (2014) p. 3174,
 949 arXiv: [1407.5066](#) [[hep-ph](#)].
- 950 [84] M. Klasen, M. Pohl, and G. Sigl, *Indirect and direct search for dark matter*,
 951 *Prog. Part. Nucl. Phys.* **85** (2015) p. 1, arXiv: [1507.03800](#) [[hep-ph](#)].

- 952 [85] L. Evans and P. Bryant, *LHC Machine*, JINST **3** (2008) S08001.
- 953 [86] V. Shiltsev, “Accelerator Physics and Technology,” 2016,
954 URL: [https://indico.fnal.gov/sessionDisplay.py?sessionId=3&](https://indico.fnal.gov/sessionDisplay.py?sessionId=3&confId=11505#20160811)
955 [confId=11505#20160811](https://indico.fnal.gov/sessionDisplay.py?sessionId=3&confId=11505#20160811).
- 956 [87] *LEP design report*, Copies shelved as reports in LEP, PS and SPS libraries,
957 Geneva: CERN, 1984, URL: <https://cds.cern.ch/record/102083>.

The Standard Model

In this appendix, we provide a brief overview of the basic ingredients involved in construction of the Standard Model Lagrangian : quantum field theory, symmetries, and symmetry breaking.

Quantum Field Theory

In this section, we provide a brief overview of the necessary concepts from Quantum Field Theory (QFT).

In modern physics, the laws of nature are described by the “action” S , with the imposition of the principle of minimum action. The action is the integral over the spacetime coordinates of the “Lagrangian density” \mathcal{L} , or Lagrangian for short. The Lagrangian is a function of “fields”; general fields will be called $\phi(x^\mu)$, where the indices μ run over the space-time coordinates. We can then write the action S as

$$S = \int d^4x \mathcal{L}[\phi_i(x^\mu), \partial_\mu \phi_i(x^\mu)] \quad (9.1)$$

where we have an additional summation over i (of the different fields). Generally, we impose the following constraints on the Lagrangian :

1. Translational invariance - The Lagrangian is only a function of the fields ϕ and their derivatives $\partial_\mu \phi$
2. Locality - The Lagrangian is only a function of one point x_μ in spacetime.

cite Yuval's
lectures
and notes
somehow

cite

- 976 3. Reality condition - The Lagrangian is real to conserve probability.
- 977 4. Lorentz invariance - The Lagrangian is invariant under the Poincaré group of
978 spacetime.
- 979 5. Analyticity - The Lagrangian is an analytical function of the fields; this is to
980 allow the use of perturbation theory.
- 981 6. Invariance and Naturalness - The Lagrangian is invariant under some internal
982 symmetry groups; in fact, the Lagrangian will have *all* terms allowed by the
983 imposed symmetry groups.
984 7. Renormalizability - The Lagrangian will be renormalizable - in practice, this
985 means there will not be terms with more than power 4 in the fields.

986 The key item from the point of view of this thesis is that of “Invariance and
987 Natural”. We impose a set of “symmetries” and then our Lagrangian is the most
988 general which is allowed by those symmetries.

989 Symmetries

990 Symmetries can be seen as the fundamental guiding concept of modern physics.
991 Symmetries are described by “groups”. . To illustrate the importance of symmetries
992 and their mathematical description, groups, we start here with two of the simplest
993 and most useful examples : \mathbb{Z}_2 and $U(1)$.

994 \mathbb{Z}_2 symmetry

995 \mathbb{Z}_2 symmetry is the simplest example of a “discrete” symmetry. Consider the most
996 general Lagrangian of a single real scalar field $\phi(x_\mu)$

$$\mathcal{L}_\phi = \frac{1}{2}\partial_\mu\phi\partial^\mu\phi - \frac{m^2}{2}\phi^2 - \frac{\mu}{2\sqrt{2}}\phi^3 - \lambda\phi^4 \quad (9.2)$$

Now we *impose* the symmetry

$$\mathcal{L}(\phi) = \mathcal{L}(-\phi) \quad (9.3)$$

997 This has the effect of restricting the allowed terms of the Lagrangian. In particular,
 998 we can see the term $\phi^3 \rightarrow -\phi^3$ under the symmetry transformation, and thus must
 999 be disallowed by this symmetry. This means under the imposition of this particular
 1000 symmetry, our Lagrangian should be rewritten as

$$\mathcal{L}_\phi = \frac{1}{2}\partial_\mu\phi\partial^\mu\phi - \frac{m^2}{2}\phi^2 - \lambda\phi^4 \quad (9.4)$$

1001 The effect of this symmetry is that the total number of ϕ particles can only change
 1002 by even numbers, since the only interaction term $\lambda\phi^4$ is an even power of the field.
 1003 This symmetry is often imposed in supersymmetric theories, as we will see in Chapter
 1004 3.

1005 **$U(1)$ symmetry**

1006 $U(1)$ is the simplest example of a continuous (or *Lie*) group. Now consider a theory
 1007 with a single complex scalar field $\phi = \text{Re } \phi + i \text{Im } \phi$

$$\mathcal{L}_\phi = \delta_{i,j} \frac{1}{2} \partial_\mu \phi_i \partial^\mu \phi_j - \frac{m^2}{2} \phi_i \phi_j - \frac{\mu}{2\sqrt{2}} \phi_i \phi_j \phi_k - \lambda \phi_i \phi_j \phi_k \phi_l \quad (9.5)$$

1008 where $i, j, k, l = \text{Re}, \text{Im}$. In this case, we impose the following $U(1)$ symmetry
 1009 : $\phi \rightarrow e^{i\theta} \phi, \phi^* \rightarrow e^{-i\theta} \phi^*$. We see immediately that this again disallows the third-order
 1010 terms, and we can write a theory of a complex scalar field with $U(1)$ symmetry as

$$\mathcal{L}_\phi = \partial_\mu \phi \partial^\mu \phi^* - \frac{m^2}{2} \phi \phi^* - \lambda (\phi \phi^*)^2 \quad (9.6)$$

1011 Local symmetries

1012 The two examples considered above are “global” symmetries in the sense that the
 1013 symmetry transformation does not depend on the spacetime coordinate x_μ . We know
 1014 look at local symmetries; in this case, for example with a local $U(1)$ symmetry, the
 1015 transformation has the form $\phi(x_\mu) \rightarrow e^{i\theta(x_\mu)}\phi(x_\mu)$. These symmetries are also known
 1016 as “gauge” symmetries; all symmetries of the Standard Model are gauge symmetries.

There are wide-ranging consequences to the imposition of local symmetries. To begin, we note that the derivative terms of the Lagrangian 9.2 are *not* invariant under a local symmetry transformation

$$\partial_\mu \phi(x_\mu) \rightarrow \partial_\mu (e^{i\theta(x_\mu)} \phi(x_\mu)) = (1 + i\partial_\mu \theta(x_\mu)) e^{i\theta(x_\mu)} \phi(x_\mu) \quad (9.7)$$

GET THIS

RIGHT

1017 This leads us to note that the kinetic terms of the Lagrangian are also not invariant
 1018 under a gauge symmetry. This would lead to a model with no dynamics, which is
 1019 clearly unsatisfactory.
 1020

1021 Let us take inspiration from the case of global symmetries. We need to define a
 1022 so-called “covariant” derivative D^μ such that

$$D^\mu \phi \rightarrow e^{iq\theta(x_\mu)} D^\mu \phi \quad (9.8)$$

$$D^\mu \phi^* \rightarrow e^{-iq\theta(x_\mu)} D^\mu \phi^* \quad (9.9)$$

$$(9.10)$$

1023 Since ϕ and ϕ^* transform with the opposite phase, this will lead to the invariance
 1024 of the Lagrangian under our local gauge transformation. This D^μ is of the following
 1025 form

$$D^\mu = \partial_\mu - igqA^\mu \quad (9.11)$$

1026 where A^μ is a vector field we introduce with the transformation law

$$A^\mu \rightarrow A^\mu - \frac{1}{g} \partial_\mu \theta \quad (9.12)$$

1027 and g is the coupling constant associated to vector field. This vector field A^μ is
1028 also known as a “gauge” field.

1029 Since we need to add all allowed terms to the Lagrangian, we define

$$F^{\mu\nu} = A^\mu A^\nu - A^\nu A^\mu \quad (9.13)$$

1030 and then we must also add the kinetic term :

$$\mathcal{L}_{\text{gauge}} = -\frac{1}{4} F^{\mu\nu} F_{\mu\nu} \quad (9.14)$$

1031 The most general renormalizable Lagrangian with fermion and scalar fields can
1032 be written in the following form

$$\mathcal{L} = \mathcal{L}_{kin} + \mathcal{L}_\phi + \mathcal{L}_\psi + \mathcal{L}_{Yukawa} \quad (9.15)$$

1033 Symmetry breaking and the Higgs mechanism

1034 Here we view some examples of symmetry breaking. We investigate breaking of a
1035 global $U(1)$ symmetry and a local $U(1)$ symmetry. The SM will break the electroweak
1036 symmetry $SU(2) \times U(1)$, and in Chapter 3 we will see how supersymmetry must also
1037 be broken.

1038 There are two ideas of symmetry breaking

- 1039 • Explicit symmetry breaking by a small parameter - in this case, we have a small
1040 parameter which breaks an “approximate” symmetry of our Lagrangian. An
1041 example would be the theory of the single scalar field [9.2](#), when $\mu \ll m^2$ and

1042 $\mu \ll \lambda$. In this case, we can often ignore the small term when considering
 1043 low-energy processes.

1044 • Spontaneous symmetry breaking (SSB) - spontaneous symmetry breaking
 1045 occurs when the Lagrangian is symmetric with respect to a given symmetry
 1046 transformation, but the ground state of the theory is *not* symmetric with respect
 1047 to that transformation. This can have some fascinating consequences, as we
 1048 will see in the following examples

1049 Symmetry breaking a

1050 **U(1) global symmetry breaking**

Consider the theory of a complex scalar field under the $U(1)$ symmetry, or the transformation

$$\phi \rightarrow e^{i\theta} \phi \quad (9.16)$$

The Lagrangian for this theory is

$$\mathcal{L} = \partial^\mu \phi^\dagger \partial_\mu \phi + \frac{\mu^2}{2} \phi^\dagger \phi + \frac{\lambda}{4} (\phi^\dagger \phi)^2 \quad (9.17)$$

Let us write this theory in terms of two scalar fields, h and ξ : $\phi = (h + i\xi)/\sqrt{2}$.

The Lagrangian can then be written as

$$\mathcal{L} = \partial^\mu h \partial_\mu h + \partial^\mu \xi \partial_\mu \xi - \frac{\mu^2}{2} (h^2 + \xi^2) - \frac{\lambda}{4} (h^2 + \xi^2)^2 \quad (9.18)$$

First, note that the theory is only stable when $\lambda > 0$. To understand the effect of SSB, we now enforce that $\mu^2 < 0$, and define $v^2 = -\mu^2/\lambda$. We can then write the scalar potential of this theory as :

$$V(\phi) = \lambda(\phi^\dagger \phi - v^2/2)^2 \quad (9.19)$$

Minimizing this equation with respect to ϕ , we can see that the “vacuum expectation value” of the theory is

$$2 \langle \phi^\dagger \phi \rangle = \langle h^2 + \xi^2 \rangle = v^2 \quad (9.20)$$

1051 We now reach the “breaking” point of this procedure. In the (h, ξ) plane, the
 1052 minima form a circle of radius v . We are free to choose any of these minima to expand
 1053 our Lagrangian around; the physics is not affected by this choice. For convenience,
 1054 choose $\langle h \rangle = v, \langle \xi^2 \rangle = 0$.

Now, let us define $h' = h - v, \xi' = \xi$ with VEVs $\langle h' \rangle = 0, \langle \xi' \rangle = 0$. We can then write our spontaneously broken Lagrangian in the form

$$\mathcal{L} = \frac{1}{2} \partial_\mu h' \partial^\mu h' + \frac{1}{2} \partial_\mu \xi' \partial^\mu \xi' - \lambda v^2 h'^2 - \lambda v h' (h'^2 + \xi'^2) - \lambda (h'^2 + \xi'^2)^2 \quad (9.21)$$